

THE EFFECTS OF CORAL-ROUGHNESS ON
MASS TRANSFER

A THESIS SUBMITTED TO THE GRADUATE DIVISION OF THE UNIVERSITY
OF HAWAII IN PARTIAL FULFILLMENT OF THE
REQUIREMENTS FOR THE DEGREE OF

MASTER OF SCIENCE

IN

OCEANOGRAPHY

MAY 1996

By

Mark E. Baird

Thesis Committee:

Marlin J. Atkinson, Chairperson
Francis J. Sansone
Michael J. Mottl

We certify that we have read this thesis and that, in our opinion, it is satisfactory in scope and quality as a thesis for the degree of Master of Science in Oceanography.

THESIS COMMITTEE

Chairperson

Acknowledgments

My most sincere thanks go to Prof. Marlin Atkinson, whose assistance in all my endeavors in Hawaii, scientific advice and academic example have made this project possible, and thoroughly rewarding. Prof. Emeritus Keith Chave and Dr. Edith Chave ably assisted Prof. Atkinson in these matters.

I thank Prof. Bob Bilger, my supervisor at the University of Sydney, and colleague of Prof. Atkinson, for the opportunity to work under Prof. Atkinson, and the direction given on a number of technical points.

I thank committee members Frank Sansone and Mike Mottl for their thorough reviews of this thesis.

I would also like to thank Jim Fleming and Aziz Isham, whose assistance with the design and working of experiments was tireless. Experimental help was also provided by Ginny Birch, Pat Ewanchuk, Eric Hochberg, Rolf Arvidson and Charles Farley.

And to my father, a loving, supporting parent, who passed away during my time in Hawaii.

This project was funded by a grant (NA36RG0507 R/ME-2) from the NOAA Sea Grant program.

Abstract

The uptake of nutrients (nitrogen and phosphorus compounds) into coral reef communities is proposed to be limited by diffusion through a depleted boundary layer between the water and the organisms, or what is termed "mass transfer limitation". Theory from the engineering literature indicates that increased surface roughness should increase mass transfer; thus in this project the effects of coral-roughness on mass transfer were investigated experimentally using the dissolution of gypsum (plaster-of-paris) in fresh water from coral-shaped surfaces. The dissolution rate was measured as an increasing concentration of calcium ions over time in a flume of constant volume. The technique was first applied to a flat, smooth surface of gypsum over a wide range of temperatures and ionic strength. Stanton numbers (St_m , a dimensionless number giving the ratio of uptake rate per unit area to the rate of advection of the substance past the uptake surface) of experimental smooth surfaces ranged from $2.6\text{-}3.5 \times 10^{-5}$ and were within 15% of engineering literature values. Stanton numbers for coral-shaped surfaces ranged from 70×10^{-5} at 0.03 m s^{-1} to 17×10^{-5} at velocities up to 0.50 m s^{-1} , and were in general 9 ± 1 times that of smooth surfaces. The results are compared (using St_m) with flume studies on experimental coral communities, and engineering literature. The relationship between mass transfer, friction and roughness of coral-shaped gypsum surfaces can be predicted from correlations of heat transfer from sand-roughened pipes. Results presented provide confirmation of Bilger and Atkinson's (1992) model of nutrient uptake being mass-transfer limited and can be used to predict nutrient-uptake into living coral reef communities.

Table of Contents

Acknowledgments	iii
Abstract	iv
List of Tables	vii
List of Figures	viii
List of Symbols	x
Introduction	1
Background	5
Non-dimensional Analysis	8
Momentum Transport	10
Mass Transport	13
Mass Transfer of Gypsum	18
Mass Transfer on Rough Surfaces	21
Methods	25
Measurement of Momentum Transport	25
Measurement of Mass Transport	26
Measurement of Mass Transport on Coral-rough Surfaces	33
Experimental Outline	34
Results	37
Momentum Transport on Coral-rough Surfaces	37
Mass Transport on Coral-rough Gypsum Surfaces	38
Discussion	45
Momentum Transport	45

Mass Transport	46
Other Mass Transfer Studies on Coral-rough Surfaces	47
Implications for Coral Reef Ecology	53
A Changing Boundary Layer	57
Conclusions	60
Appendix A: Mass Transfer in Oscillatory Flow	61
Appendix B: Choice of Mass Transfer Model	74
Appendix C: Matlab Program for Stanton Number Calculations	78
Appendix D: Thickness of the Gypsum Coat on Coral-rough Surfaces	84
Glossary	87
References	91

List of Tables

1. Topographical profile for a coral-rough surface	37
2. Summary of experimental results	43
3. Data comparison for coral-rough surface	48

List of Illustrations

1. Illustration of flume during smooth surface experiments	14
2. Illustration of flume during coral rough surface experiments	15
3. Illustration of the derivation of the Stanton number	16
4. Illustration of roughness scales	24
5. Smooth surface momentum characteristics	26
6. Gypsum-coated coral rubble before placement in flume	29
7. Measurement of roughness for a coral assemblage	29
8. Graph of measured calcium vs. specific conductance	30
9. Specific conductance vs. time for Exp. 16	31
10. Stanton number vs. time for Exp. 4	32
11. Stanton number vs. time for Exp. 14	33
12. Roughness profile for Exp. 16	38
13. Momentum characteristics of a coral-rough surfaces	39
14. Photographs of Exp. 14 at four different times	40
15. St_m vs. U_b for Exp. 4-6, 11, 13-19	42
16. Measured St_m for Exps. 13-19 compared to literature values	50
17. Measured St_m for Exps. 13-19 compared to modified literature values	52
18. St_m vs. U_b fitted to an engineering formulation	54
19. Engineering performance of coral-rough surfaces	59
A1. Model for changing boundary layer thickness	63
A2. Boundary Layer concentration profile for Ex. 2	66
A3. Surface flux for Ex. 2	66

A4. Boundary Layer concentration profile for Ex. 3	67
A5. Surface flux for Ex. 3	68
B1. Mass Transfer Models	77
D1. Cross section of a coral-rough gypsum specimen	86

List of Symbols

A	projected area [m ²]	k _σ	standard deviation of roughness
A _c	cross sectional area [m ²]		element height [m]
a	activity	k _{1,2,..}	other roughness scales [m]
C	concentration [mol m ⁻³]	L	length [m]
c _f	friction coefficient	m _s	flux from surface [mol m ⁻² s ⁻¹]
D	diffusivity [m ² s ⁻¹]	m	molality of chemical species
D _h	hydraulic diameter [m ²]	n	quantity of chemical species
F	thermodynamic force	n	Manning roughness parameter [m ^{1/6}]
G	Gibb's free energy	P	perimeter [m]
GPE	gravitational potential energy [J]	p	pressure [Pa]
g	gravity [m s ⁻²]	Pr	Prandtl number
H	head [m]	R	universal gas constant [J K ⁻¹ mol ⁻¹]
h	height [m]	Re	Reynolds number
I	ionic strength	Re _k	Reynolds roughness number
J	flux [mol m ⁻² s ⁻¹]	s	slope [m m ⁻¹]
K	equilibrium constant	s _d	drift speed [m s ⁻¹]
KE	kinetic energy [J]	Sc	Schmidt number
k	constant	Sc _t	turbulent Schmidt number
k'	roughness element height [m]	Sh	Sherwood number
k _s	equivalent sand-grain roughness [m]	St _k	roughness Stanton number

St_m	Stanton number for mass transfer	z	valence
		α	angle of slope with horizontal
T	temperature [K]		wetted area / projected area ratio
U	velocity [$m\ s^{-1}$]	γ	activity coefficient
u^*	friction velocity [$m\ s^{-1}$]	μ	chemical potential [$J\ mol^{-1}$]
V	volume of flume [m^3]	ν	kinematic viscosity [$m^2\ s^{-1}$]
W	width [m]	ρ	density [$kg\ m^{-3}$]
x	thickness of diffusive boundary layer [m]	τ_w	wall shear stress [$N\ m^{-1}$]

Subscripts / Superscripts

b	bulk
w	wall
\emptyset	standard state
1,2,3..	chemical species
1	upstream of sample
2	downstream of sample

It seems appropriate, before so mechanically discussing the workings of coral reef ecosystems, to dwell briefly on the words of one of the first to marvel at the simple existence of coral reefs:

"The organic forces separate the atoms of carbonate of lime, one by one, from the foaming breakers, and unite them into a symmetrical structure. Let the hurricane tear up its thousand huge fragments; yet what will that tell against the accumulated labour of myriads of architects at work night and day, month after month ? Thus do we see the soft gelatinous body of a polypus, through the agency of the vitals laws, conquering the great mechanical power of the waves of an ocean which neither the art of man nor the inanimate works of nature could successfully resist".

Charles Darwin, Voyage of the Beagle (1836)

Introduction

The transfer of dissolved compounds to and from a solid surface is fundamental to many processes in engineering, biology, chemistry and geology. Examples in these disciplines include industrial electrochemical processes, the growth and metabolism of organisms, the dissolution and precipitation of minerals, and the formation and destruction of geological features.

In a turbulent flow, when the reaction rate at the surface is fast compared to diffusion through the fluid, transfer rate between the fluid and the surface becomes dependent on the velocity of the fluid. This velocity dependence has been observed in natural environments (Atkinson and Bilger, 1992; Jumars and Nowell, 1984) and laboratory setups (Selman and Tobias, 1978; Grifoll et al., 1986). Under the condition of velocity dependence, transfer rate is generally considered to be mass-transfer limited.

Roughness of the surface can influence the turbulence and velocity of the fluid near the surface. Roughness is ubiquitous in natural environments, occurring on both organic and inorganic surfaces. The investigation of the transfer of chemical species to and from a rough living surface has been conducted in terrestrial environments (Raupach and Thom, 1981), and marine systems (Boudreau and Guinasso, Jr., 1978; Atkinson and Bilger, 1992; Bilger and Atkinson, 1995; Thomas and Atkinson, 1996). A strong correlation between flow characteristics such as bulk velocity and turbulence with metabolic rate has been a theme of the above cited studies.

A characteristic common to most of the laboratory studies in engineering literature is an ordered rough surface, with only one scale of relatively small roughness element heights (Dawson and Trass, 1972; Tantirige and Trass, 1984; Reynolds, 1975;

Lee and Soliman, 1977; Weber, 1979; Steward 1987; Grifoll et al., 1986; Herrero et al., 1991,1994). Naturally rough surfaces, such as those studied in biology (Atkinson, 1992) and geology (Boudreau and Guinasso, Jr., 1978), are typically disorderly, often with large variation in roughness scales, and large surface area to projected area ratios.

Bilger and Atkinson (1992) attempted to use the engineering literature to explain field measurements for the uptake of phosphate and ammonia on coral reef flats. They concluded that "regardless of the mechanism, it has been shown that P [phosphate] uptake on a large coral reef flat is anomalously fast when compared with existing engineering literature on mass transfer." The velocity dependence of mass transfer (Atkinson and Bilger, 1992) indicates that the rate limiting step is diffusion through the boundary layer. In other words, the nutrient uptake is mass-transfer limited. The "anomalously fast" transfer rate suggests a difference in the boundary layer structure between the ordered rough laboratory environments and rough field environments.

Atkinson (1992) applied mass-transfer limited relationships from Bilger and Atkinson (1992) and Atkinson and Bilger (1992), to obtain good agreement between predicted and measured productivity of Enewetak Atoll reef flats. Furthermore, Thomas and Atkinson (1996) experimentally showed a strong correlation between uptake-rates of ammonia, energy dissipated and roughness of four different reef communities, confirming ammonium-uptake is mass transfer limited.

The higher rates of mass transfer observed in natural environments compared to engineering experiments could be geometric in origin, such as: different scales of roughness (Atkinson, 1992); the proposed fractal nature of the surface (Bilger and Atkinson, 1992); a different surface area to projected area ratio; or a preference for more

effective shapes. These geometric phenomena would also be present on an inorganic surface of the same shape with a dissolution rate which is mass-transfer limited.

Alternatively, the enhancement could be due to uniquely biological structures such as: "surface slimes" or the "action of cilia and flagella of microscopic organisms" (Bilger and Atkinson, 1992); the elastic properties of the surface (Peskin and McQueen, 1995); or a non-Newtonian mucus layer. An enhancement due to biological structures in the boundary layer, however, would not be observed on an inorganic mineral surface.

The commercial grade of gypsum, plaster-of-paris, can be molded into coral shapes, and the dissolution rate of gypsum in water is mass-transfer limited (Barton and Wilde, 1971). Thus the goal of this research is to use an analog, the dissolution of gypsum, to investigate the effects of coral-roughness on mass transfer, and to compare these results with measurements of nutrient-uptake on experimental and field coral communities. The results may also indicate the feasibility of similar mass transfer studies on disordered rough surfaces throughout the natural sciences.

The fluxes of different chemical species in varying mediums and concentrations can be compared using a set of non-dimensional parameters common to engineering literature. Fluxes are described by a rate coefficient called the Stanton number, and are compared at similar flow conditions, as measured by the friction factor, Reynolds roughness number and Schmidt number. The engineering methods provide a direct comparison of the fluxes on a living coral community to an inorganic coral-shaped surface.

The experimental flume used in this study was geometrically similar to the flume used for the Atkinson and Bilger experiments of 1992-1995, and those used in many engineering studies.

Background

As fluid flows past a stationary wall a gradient in velocity is observed from the wall to the center of the flow. The region of the flow where the velocity changes from that at the wall to 99% of the freestream flow is called the momentum boundary layer. Natural fluid flows are often turbulent. In turbulent flows, the velocity gradients are steep at the wall, and the momentum boundary layer is thin (John and Haberman, 1988). Turbulence is responsible for convective transport of momentum (and, as shall be seen later, heat and mass) which is orders of magnitude quicker than diffusive transport. The transport of momentum by turbulence quickly homogenizes the fluid away from the wall. As a result, there are only small velocity gradients within the bulk flow where turbulence proliferates, but steep gradients close to the wall, where momentum is transported by diffusion.

Turbulence is also responsible for convective transport of heat and mass transfer, which is orders of magnitude faster than diffusive mass and heat transfer. In a turbulent flow, dissolved compounds in the bulk fluid move equally in all directions, resulting in a well-mixed volume, with no chemical potential gradient. Close to the wall, however, velocity decreases, and all transport is by diffusion. Thus, a fast rate of input or removal of dissolved compounds at the wall creates a chemical potential gradient. For a chemical flux to occur from the bulk volume to the surface, it must be transported by diffusion down the chemical potential gradient.

The diffusive sublayer is a thin region close to the wall where transport is down chemical potential gradients towards the wall. The outer extension of the diffusive sublayer is set by the point at which the fluid velocity perpendicular to the wall

approaches zero. As water velocity across a surface is increased, the flow becomes more turbulent, the diffusive sublayer becomes thinner, and the chemical potential gradient is increased.

The diffusive sublayer thickness is therefore set by the physical - not chemical - characteristics of the flow. Mass transport to the wall in the diffusive sublayer can only occur by diffusion, which is orders of magnitude slower than convective transport within the bulk fluid. The transport of dissolved compounds to and away from the surface is determined by the slowest or rate limiting step: diffusion through the diffusive sublayer.

The chemical potential, μ , in a one-chemical system is defined (Atkins, 1994) as:

$$\mu = \mu^\ominus + RT \ln(p/p^\ominus) \quad (1)$$

where $R = 8.315 \text{ [J K}^{-1} \text{ mol}^{-1}]$ is the universal gas constant, T is temperature [K], p is pressure, and \ominus signifies a property at a standard state. In a multi-component system, the chemical potential of one species is a function of changing chemical potential of other components as well. The chemical potential of a chemical species in a infinite species system is most generally defined as:

$$\mu_1 = \left(\partial G / \partial n_1 \right)_{p, T, n_2, n_3, \dots} \quad (2)$$

where G is total Gibb's free energy, and n_1 is the quantity of species 1 in solution.

Diffusion is the movement of a chemical species from one energy level to another energy level a distance away, and will be considered as a thermodynamic force per mole, $F \text{ [J m}^{-1} \text{ mol}^{-1}, \text{ kg m s}^{-1} \text{ mol}^{-1}, \text{ or N mol}^{-1}]$. We can now write the force F as a change in chemical potential per unit length, δx :

$$F = -\left(\partial \mu / \partial x \right)_{p, T, n_2, n_3, \dots} \quad (3)$$

Another force that can exist in a chemical potential gradient is due to an electric field. In the case of charge separation of ion species without an external electric field being applied, such as found in this study, the force will be relatively small, and will not be included in the analysis. To work towards a more familiar relationship for diffusion, we return to a single component system, without an electric field, and we obtain from Eq. 1:

$$\mu = \mu^\ominus + RT \ln a \quad (4)$$

where the activity, a , of the one species is defined as the 'effective' mole fraction or pressure, relative to that a standard state. i.e., $a = (p/p^\ominus)$.

The thermodynamic force is the gradient in chemical potential. Substituting Eq. 4 into Eq. 3 gives:

$$F = -(d/dx)\{\mu^\ominus + RT \ln a\} = RT(\partial \ln a / \partial x)_{p,T} \quad (5)$$

The activity is given by: $a = \gamma C$ where γ is the activity coefficient. In an ideal solution, or when the dissolved chemical species is infinitely dilute, $\gamma = 1$, and $a = C$ [mol m⁻³]. Since $(d/dx) \ln C = (1/C)(dC/dx)$, (5) becomes:

$$F = -(RT/C)(\partial C / \partial x)_{p,T} \quad (6)$$

In the presence of a chemical potential gradient, the thermodynamic force, F , results in the relative motion of the chemical species. A force balance may be constructed by balancing the thermodynamic force (Eq. 6) moving Gibb's free energy down the chemical potential gradient, with the viscous drag that opposes the motion. The viscous drag will be proportional to the viscosity of the solvent and the atomic radius of the solute. The balance is achieved at a drift speed, s_d , proportional to F . A drift speed, s_d [m

s^{-1}], relative to a volume of solution [m^3], gives rise to a flux, $J = s_d C = kFC$ (where J is a flux [$mol\ m^{-2}\ s^{-1}$], and k is a constant [$m^2\ mol\ J^{-1}\ s^{-1}$]). Solving for the flux, J , gives:

$$J = -(kRT)\left(\frac{\partial C}{\partial x}\right)_{p,T} \quad (7)$$

Eq. 7 has the form of Fick's 1st law, where $D_{12} = kRT$ [$m^2\ s^{-1}$], the diffusion coefficient of species 1 through species 2, is a constant. Fick's 1st law is often a good approximation of the diffusion of chemical species down chemical potential gradients.

The dissolution of gypsum in a fluid of changing ionic strength, I , and temperature, however, departs significantly from ideal Fick's law behavior with constant D_{12} . The methodology to quantify the non-ideal behavior of the mass transfer of a chemical species to and from a rough surface in a turbulent flow is the focus of the rest of this section, and lays the foundation for using the dissolution of gypsum as an experimental analogue for nutrient uptake on coral reefs.

Non-dimensionless Analysis

Quantities that influence the transport-rate of chemical species¹ (J in the previous sections, but from now on referred to as m_s) to and from a surface include:

1. Kinematic viscosity of the fluid, ν [$m^2\ s^{-1}$].
2. Density of the fluid, ρ [$kg\ m^{-3}$]
3. Ratio of the volume of the flume to the projected area of the sample, V/A [m].
4. Diffusivity of the chemical species 1 through species 2, D_{12} [$m^2\ s^{-1}$].
5. Chemical potential gradient, $\mu_w - \mu_b$, or more simply the concentration

¹ The effects of temperature and ionic strength on mass transfer can be measured indirectly as a change in the viscosity, density and diffusivity of the fluid.

gradient, $C_w - C_b$ [mol m^{-3}].

6. Bulk velocity of fluid, U_b [m s^{-1}].

7. Roughness height, k [m].

To compare the dissolution of gypsum to nutrient uptake on coral reefs we must take into account the seven above-listed variables (v , ρ , V/A , D , $C_w - C_b$, U_b and k). To experimentally investigate the effect of each variable would be a very lengthy and expensive process. For example, to take 10 measured points for each variable while holding the other variables constant would require 10^7 measurements. Furthermore, a correlation with seven variables would be overly complex and prone to error propagation.

Fundamental fluid dynamics texts (John and Haberman, 1988) detail a method (Buckingham-Pi theorem²) of reducing the number of physical variables required to describe a mass transfer on a rough surface. The above seven quantities contain only three fundamental units: mass, length, and time. It is therefore predicted by the Buckingham-Pi theorem that $7 - 3 = 4$ dimensionless groups of variables will describe the mass-transfer rates. Dipprey and Sabersky (1963) use the Stanton number, St_m , the friction coefficient c_f , the Schmidt number, Sc , and the Reynolds roughness number, Re_k . This leaves us with only four dimensionless groups which influence mass transfer.

The following theoretical development will derive these dimensionless groups, and how they can be calculated from measurable quantities. With this achieved, we will be able to compare the dissolution of gypsum from coral-shapes to nutrient uptake on coral reefs.

² The description and justification of this method are well detailed in most fundamental fluid dynamics texts.

Momentum Transport

Moving water in a recirculating flume must maintain a balance of the kinetic energy (KE), gravitational potential energy (GPE) and energy dissipation by friction. In the absence of an acceleration of the volume of water, and in order to conserve mass, the KE of the fluid will not change over time. The friction dissipation must therefore be balanced by a loss in GPE. The loss in GPE over a distance results in a slope on the surface of the water (Fig. 1). The rougher the surface, the larger the friction dissipation by the surface, and therefore the greater the loss in GPE required to balance the loss of energy due to friction. The greater change in GPE is observed as a steeper slope (Fig. 2).

For steadily flowing water in the empty flume (Fig. 1), a force balance on a volume of fluid in a flume with friction on the bottom and sides is summarized as:

loss in GPE = friction dissipated (in terms of τ_w or c_f)

$$\rho g L W h s = \tau_w (L W + 2 L h) = \left(\frac{c_f}{2}\right) \rho U_b^2 (L W + 2 L h) \quad (8)$$

where ρ is density [kg m^{-3}]; g is acceleration due to gravity [m s^{-2}]; L , W , h are the length, width and height [m] of the volume of water; s is the slope of the water [m m^{-1}]; and τ_w is the wall shear stress [N m^{-2}]. c_f is the dimensionless friction coefficient, defined as:

$$c_f \equiv \frac{\tau_w}{\rho U_b^2 / 2} \quad (9)$$

The friction coefficient, c_f , is a dimensionless measure of the shear stress arising from both skin friction and form drag. The experimental flume is filled to $W \cong 2h$, and solving for c_f from Eqs. 8 & 9:

$$c_f = \frac{2gWhs}{U_b^2(W+2h)} \cong \frac{gWs}{2U_b^2} \quad (10)$$

From readily measurable variables, the friction coefficient can now be obtained. The friction coefficient, along with other dimensionless parameters, has been used in empirical correlations for estimating other property transport phenomena such as heat transfer in roughened pipes (Dippery and Sabersky, 1963), mass transfer on grooved surfaces (Dawson and Trass, 1972), and nutrient-uptake on coral reefs (Bilger and Atkinson, 1992).

For flow in the flume, the Reynolds number, the ratio of inertia forces to viscous forces, is defined as:

$$Re \equiv \frac{U_b D_h}{\nu} \quad (11)$$

where U_b [$m\ s^{-1}$] is the bulk velocity of the fluid over the surface, D_h [m] is the hydraulic diameter, and ν [$m^2\ s^{-1}$] is the kinematic viscosity. The hydraulic diameter of the flume is given as (Kays and Crawford, 1993):

$$D_h = \frac{4A_c}{P} \quad D_{h,smooth} = \frac{4 \times 0.4 \times 0.2}{0.4 + 0.2 + 0.2} = 0.4 \quad (12)$$

where A_c [m^2] is the cross-sectional area of the flow, and P [m] the perimeter of the flow experiencing a shear-stress. For the empty flume, the friction coefficient of the air-water interface, $c_{f,air}$, will be small compared to the sides, $c_{f,side}$, and the bottom, $c_{f,bottom}$. The hydraulic diameter for this smooth flow is $D_h = 0.4$. The Reynolds number can now be calculated, given D_h , U_b , ρ , and μ .

The Manning formula [John and Haberman, 1988] is an experimentally derived relationship for the slope of the water surface as a function of velocity:

$$U_b = \frac{0.820}{n} \left(\frac{A_c}{P} \right)^{2/3} \sqrt{\sin \alpha} \quad (13)$$

where the Manning roughness parameter is $n = 0.01 \text{ m}^{1/6}$ for a smooth surface, and α is the angle of the slope with the horizontal.

When rough objects are placed in the bottom of the flume (Fig. 2), the friction due to the side walls becomes small compared with the bottom. The flow acts as though the walls were not there because the presence of the walls has only a small effect on flow compared to the bottom. This is a similar condition to an open channel, such as a reef flat. A similar equation development as above for an open channel - describing the flume with a rough bottom - is given by Bilger and Atkinson (1992), with Eqs. 8,10, & 12 becoming:

$$\rho g L W h s = \tau_w L W = \left(\frac{c_f}{2} \right) \rho U_b^2 L W \quad (14)$$

$$c_f = \frac{2 g h s}{U_b^2} \quad (15)$$

$$D_{h,rough} = 4h = 0.8m \quad (16)$$

Bilger and Atkinson (1992) choose Haaland's (1983) relationship, modified for an open channel, to describe the friction coefficient in terms of roughness heights, height of the water, and the Reynolds number. Haaland's relationship gives a similar result to the Manning equation, but is specific to open channel type flows:

$$\left(c_f / 2 \right)^{-1/2} = -5.1 \log_{10} \left[\frac{6.9}{\text{Re}} + \left(\frac{k_s}{14.8h} \right)^{1.11} \right] \quad (17)$$

where k_s is the equivalent sand-grain roughness, as defined by Schlichting (1955). Both the Manning and Haaland relationships provide useful comparisons between the performance of the flume used in this study and those of previous investigators.

Mass Transport

The primary aim of this study is to investigate the mass transfer characteristics of an inorganic coral-shaped surface in characterized laboratory flows. As shown in Fig. 3, conservation of mass of a chemical species, given no sources or sinks within the fluid, requires that:

$$\text{Flux}_{\text{out, bottom}} = \text{Flux}_{\text{in}} - \text{Flux}_{\text{out, front}} \quad (18)$$

Using the notation in Fig. 3, Eq. 18 requires:

$$-mWdx = U_b hWdC_b \quad (19)$$

where C_b [mol m^{-3}] is the average bulk concentration, C_w is the concentration at the wall, and dx is an elemental length of the fluid volume. To compare the flux of different chemicals over different concentration gradients, a non-dimensional flux, the Stanton number (St_m) is introduced (Eq. 20).

Figure 1. Illustration of the flume during a smooth surface experiment. The velocity is measured by timing a drogue placed in the flow. The slope is measured by a pressure drop across the reactive surface. The slope balances the friction dissipation with a loss in gravitational potential energy.

Figure 2. Illustration of flume during coral-rough surface experiments. The slope of the water is greater than that over a smooth surface, due to a higher frictional resistance of the coral. Roughness is measured at 1 cm intervals along the sample.

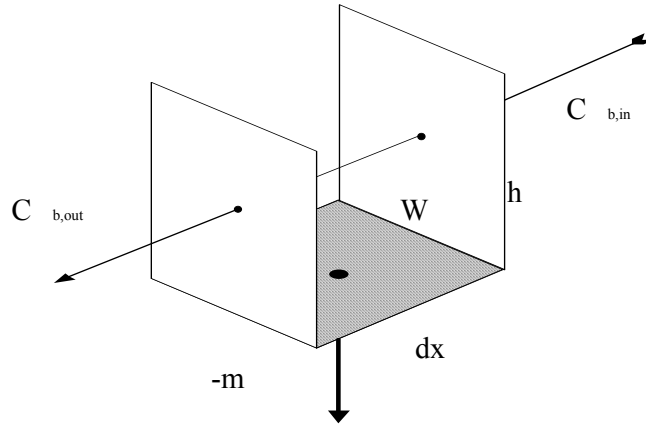


Figure 3. The Stanton number is defined as the advection of a substance past the surface divided by the uptake of that substance on the reacting surface (Eq. 20).

$$St_m = \frac{m_s}{U_b(C_b - C_w)} \quad (20)$$

The St_m can be thought of as the ratio of the uptake rate, (m_s , [$\text{mol m}^{-2} \text{s}^{-1}$]) to the rate of a the substance that is carried, or advected, past the uptake surface ($U_b(C_b - C_w)$). Using the conservation of mass (Eq. 19), and our newly defined St_m (Eq. 20), we obtain:

$$dC_b = -m_s / U_b (dx / h) = -St_m (C_b - C_w) dx / h \quad (21)$$

Experimentally, a strong correlation between momentum transport and mass transport is observed (Kays and Crawford, 1993). Thus, the Schmidt number (Sc), a non-dimensional ratio of the diffusivity of momentum and mass is used in equations to predict St_m :

$$Sc = \frac{\nu}{D_{12}} \quad (22)$$

Sc is therefore the ratio of molecular diffusivity of momentum, ν [$\text{m}^2 \text{s}^{-1}$], to molecular diffusivity of mass, D_{12} [$\text{m}^2 \text{s}^{-1}$]. Diffusivity is a function of ionic strength, I , and temperature, T [K]. Ionic strength is defined (Atkins, 1994) as:

$$I = \frac{1}{2} \sum_j (m_j / m^\ominus) z_j^2 \quad (23)$$

where m_j = molality species j , m^\ominus = molality of solute, and z_j^2 = valence of species j .

To compare measured St_m from different experiments and to other studies, Sc of the chemical species at the time of measurement must be determined. Sc is strongly a function of temperature and ionic strength, and both must therefore be measured throughout experimentation.

Given identical flow conditions (and therefore friction factor c_f), it should be expected that St_m will be a function of Sc only. Therefore, we can study the fluxes of one chemical species by substituting a different chemical of measurable Sc under the same flow conditions. A comparison of St_m for a smooth surface has been made by Steward (1987) fitting data of Shaw and Hanratty (1977) of $1730 < Sc < 37200$, and infinite dilution to formulate:

$$St_{m,smooth} = \sqrt{c_f/2} (0.0575Sc^{-2/3} + 0.1184Sc^{-1}) \quad (24)$$

As suggested above, for identical c_f , St_m is a function of Sc only. It should be noted that the use of Eq. 24 required extrapolation to $Sc = 1250$.

The non-ideal effects of ionic strength and temperature variation on diffusion (Eq. 1-7) in general have not been applied in mass transfer studies. Thus using a changing diffusivity in the Sc (Eq. 22) is unique. This combination of physical chemistry and engineering mass-transfer formulations provides the basis for experimentation on naturally rough surfaces using the dissolution of gypsum.

Stanton numbers calculated from the dissolution of coral-shaped gypsum can now be compared to the flux of nutrients to a live coral community. This fulfills the goal of

the experimentation: to determine if the origin of the mass transfer enhancement is geometric or biological. We need to calculate the Sc number of gypsum in fresh water of changing temperature and ionic strength. We must also learn to quantify flow conditions over a coral-rough surface in terms of Re_k and c_f .

Mass Transfer of Gypsum

As outlined in the introduction, the dissolution of coral-shaped gypsum will be compared to the uptake of nutrients on living coral. The dissolution of a mineral, forming two or more ions, differs from the uptake of a single compound, such as ammonia. These differences are discussed and corrected for in the following section.

When gypsum ($CaSO_4 \cdot 2H_2O$) dissolves from a surface, Ca^{2+} and SO_4^{2-} ions are released in equal quantities into solution. With an equal flux of both ions, the bulk concentrations will be approximately equal:

$$[Ca^{2+}]_b = [SO_4^{2-}]_b \quad (25)$$

However, the rate of diffusion of the two species through water is different, Ca^{2+} being the slower of the two (Li and Gregory, 1974). The thickness of the diffusive sublayer, x , is set by the point of no vertical motion of fluid in the momentum boundary layer, and applies equally to both chemical constituents. As a result, to maintain the same flux, bulk concentration and diffusive sublayer thickness, the chemical potential gradient of Ca^{2+} must be greater than SO_4^{2-} .

From Eq. 20, we can derive an equal flux of Ca^{2+} and SO_4^{2-} over a chemical potential gradient as:

$$m = St_{m,Ca} U_b ([Ca^{2+}]_w - [Ca^{2+}]_b) = St_{m,SO_4^{2-}} U_b ([SO_4^{2-}]_w - [SO_4^{2-}]_b) \quad (26)$$

where the effects of changing ionic strength and temperature (making concentration gradient \neq chemical potential gradient) are contained within the calculation of Sc (Eq. 22), St_m being a function of Sc (Eq. 24).

Dawson and Trass (1972) experimentally show for a chemical species with high Schmidt numbers that:

$$Sh = 0.0153 Re^{0.88} Sc^{0.32} \quad (27)$$

where Sh = Sherwood number. The Sherwood number is the dimensionless concentration gradient at the surface, and provides a measure of the convective mass transfer occurring from the surface (Incropera and de Witt, 1990). Since $St_m = Sh / ReSc$, the ratio of Stanton numbers for Ca^{2+} and SO_4^{2-} is given by:

$$\frac{St_{m,Ca^{2+}}}{St_{m,SO_4^{2-}}} = \frac{0.0153 Re^{-0.12} Sc_{Ca^{2+}}^{-0.68}}{0.0153 Re^{-0.12} Sc_{SO_4^{2-}}^{-0.68}} = \frac{\left(\nu/D_{Ca^{2+}}\right)^{-0.68}}{\left(\nu/D_{SO_4^{2-}}\right)^{-0.68}} = \frac{D_{Ca^{2+}}^{0.68}}{D_{SO_4^{2-}}^{0.68}} = \left(\frac{7.93 \times 10^{-10}}{10.7 \times 10^{-10}}\right)_{inf\ dilution}^{0.68} = 0.816 \quad (28)$$

where the diffusivity of Ca^{2+} and SO_4^{2-} at infinite dilution and at 25°C are given by Li and Gregory (1974). Now, for the equal flux condition to be met, using Eq. (26), canceling the bulk velocity U_b , and using the ratio of Stanton numbers in terms of diffusivity obtained from (28), we arrive at:

$$\frac{D_{Ca^{2+}}^{0.68}}{D_{SO_4^{2-}}^{0.68}} = \frac{\left([SO_4^{2-}]_W - [SO_4^{2-}]_b\right)}{\left([Ca^{2+}]_W - [Ca^{2+}]_b\right)} \quad (29)$$

Substituting the equal bulk concentration condition (Eq. 25) and solving for $[Ca^{2+}]_b$ reveals:

$$\left(1 - \frac{D_{Ca^{2+}}^{0.68}}{D_{SO_4^{2-}}^{0.68}}\right) [Ca^{2+}]_b = [SO_4^{2-}]_w - \frac{D_{Ca^{2+}}^{0.68}}{D_{SO_4^{2-}}^{0.68}} [Ca^{2+}]_w \quad (30)$$

The equilibrium constant at saturation, $K(T)$, of gypsum in fresh water, atmospheric pressure and varying temperatures is reasonably well known (Hardie, 1967). Since the wall is assumed to be at saturation:

$$K(T) = [SO_4^{2-}]_w [Ca^{2+}]_w \quad (31)$$

Substituting Eq. 31 into Eq. 30 gives the quadratic equation:

$$\frac{D_{Ca^{2+}}^{0.68}}{D_{SO_4^{2-}}^{0.68}} [Ca^{2+}]_w^2 + \left(1 - \frac{D_{Ca^{2+}}^{0.68}}{D_{SO_4^{2-}}^{0.68}}\right) [Ca^{2+}]_b [Ca^{2+}]_w - K(T) = 0 \quad (32)$$

Since $[Ca^{2+}]_b$ and $K(T)$ are measured and calculated respectively, the positive root of Eq. 32 gives the value for $[Ca^{2+}]_w$. With this we can then calculate the concentration gradient using $[Ca^{2+}]_b$. By measuring velocity, U_b , and changes in $[Ca^{2+}]_b$ over time per unit area to obtain a flux, the Stanton number, St_m , can be calculated. As the ratio of diffusivity changes with temperature and ionic strength, and as $K(T)$ is also a function of temperature, it is necessary to solve Eq. 32 at each time interval throughout the experiment. So to obtain the St_m and Sc numbers as derived above, we require the equilibrium constant, temperature, bulk velocity, kinematic viscosity, density, and Ca^{2+} concentration in solution.

Mass Transfer on Rough Surfaces

The quantification of roughness is difficult. Surface area estimation is dependent on the resolution of measurement (i.e., the area of the smallest surface feature which can be measured). For example, a fractal is an object of infinite surface area, because an infinitely fine resolution is defined. The choice of a roughness scale is also confusing

because the very nature of the disordered roughness is to have many different scales of roughness. I will choose between two of the most commonly used roughness measures, and discuss the limitations of my choice later.

The major two non-dimensional parameters that have been used to describe surface geometry in engineering literature are wetted area to projected area ratio, α , and the Reynolds roughness number, Re_k :

$$\alpha = \frac{\text{wetted} \cdot \text{surface} \cdot \text{area}}{\text{projected} \cdot \text{wall} \cdot \text{area}} \quad (33)$$

$$Re_k \equiv \frac{u_* k}{\nu} \quad (34)$$

where the friction velocity, u_* , is defined by:

$$u_* = \sqrt{\tau_w / \rho} = U_b \sqrt{c_f / 2} \quad (35)$$

and k is a roughness scale such as average roughness element height (k') or sand-grain roughness (k_s). While α is perhaps the most appealing to use, Dawson and Trass (1972) have shown that for geometrically similar surfaces (i.e., equal α) in the same flow regime, St_m numbers differ. As a result, Re_k has been more successfully employed, and will be the used as the roughness measure in this paper.

This study will use the standard deviation of average roughness element height, k_σ , as it is the best measure of the changing height of coral heads, especially when the heads are packed together. The difference between using k_σ and k' (Fig. 4) can only be a maximum of 3% of the St_m . To be consistent, I have used k_σ on the data sets of Thomas and Atkinson (1996), Larned and Atkinson (1996) and this study (Fig. 17).

Dipprey and Sabersky (1963) developed correlations for heat and momentum transfer in sand-roughened tubes. The geometric similarity between tubes and the experimental flume is shown by Bilger and Atkinson (1992). When the rate limiting step of transfer is known to be diffusion, heat transfer and mass transfer are analogous. The dimensionless group, Pr , is the ratio of diffusive momentum transfer to diffusive heat transfer (just as the Sc number is momentum transfer to mass transfer), and can be used interchangeably with the Sc number. Bilger and Atkinson (1992) summarize the Dipprey and Sabersky (1963) correlation as:

$$St_{m,rough} = (c_f / 2) / \left[Sc_t + \sqrt{(c_f / 2) / St_k} \right] \quad (36)$$

where Sc_t = turbulent Sc number in the outer boundary layer and is approximated as 0.9, and St_k , the roughness Stanton number, is defined for $70 \leq Re_k \leq 2,400$ as:

$$St_k^{-1} = 5.19 Re_k^{0.2} Sc^{0.44} - 8.48 \quad (37)$$

Eq. 36 now gives the $St_{m,rough}$ as a function of the Sc , and geometric parameters Re_k and c_f . To calculate Sc , Re_k , and c_f we need to measure bulk velocity, U_b , hydraulic diameter, D_h , roughness height, k , the slope of the water surface, s , temperature, T , concentration of calcium ions, $[Ca^{2+}]_b$, water height, h , and the volume to surface area ratio of the flume. With the measurement of these variables over time, we can compare the dissolution of a coral-shaped gypsum surface to the uptake of nutrients on coral communities.

Figure 4. Illustration of roughness scales. This study uses k_{σ} as a roughness scale, as it provides the best measure of the changing height of the roughness elements.

Methods

A recirculating flume (Fig. 1-2) with a volume of 2.3 m^3 and channel dimensions $0.4 \text{ m} \times 0.2 \text{ m} \times 24 \text{ m}$ was used for all experiments. Fresh water was recirculated using a variable speed pump. The projected planar surface area of smooth (and flat) and coral-rough surfaces varied from $0.8\text{-}3.2 \text{ m}^2$, giving a volume to projected surface area ratio of $0.72\text{-}2.9 \text{ m}$. The bulk water velocity (U_b) of the flume was calculated from the mean of 10 measurements of the time for a drogue to travel over 1 or 2 m of sample. The flume contained flow straighteners to dampen production of turbulence through the motor and turning sections. For further flume design considerations, see Atkinson and Bilger (1992).

Measurement of Momentum Transport

The slope, s [m m^{-1}], of the water was determined by measuring the relative height difference over 9 m. Two 1.6 mm holes were drilled in the base of the flume 9 m apart. 'Tygon' tubing ran from each hole to a central point, where the water height difference was measured on a vernier scale to the nearest 0.1 mm (Figs. 1 & 2). The height of the water at the vernier scale will be exactly the same as that at the holes, provided that the water in the tubes is of identical density. The tubing was flushed before reading, to avoid gas build up or thermal gradients, either of which changes the average density of the fluid within the tube. The measured water height difference for 2 m samples of coral-rough surface included a height drop over 7 m of empty flume. Eq. (38) was used to calculate the equivalent head difference (ΔH) over 9 m of coral-rough surface.

$$\Delta H_{rough,9m} = \frac{9}{2} (\Delta H_{measured,9m} - \Delta H_{smooth,7m}) \quad (38)$$

Three measurements of height difference were averaged to obtain the slope at each velocity for every experiment. Measured head difference can then be compared to predicted head difference (Fig. 5) using the Manning formula (John and Haberman, 1988).

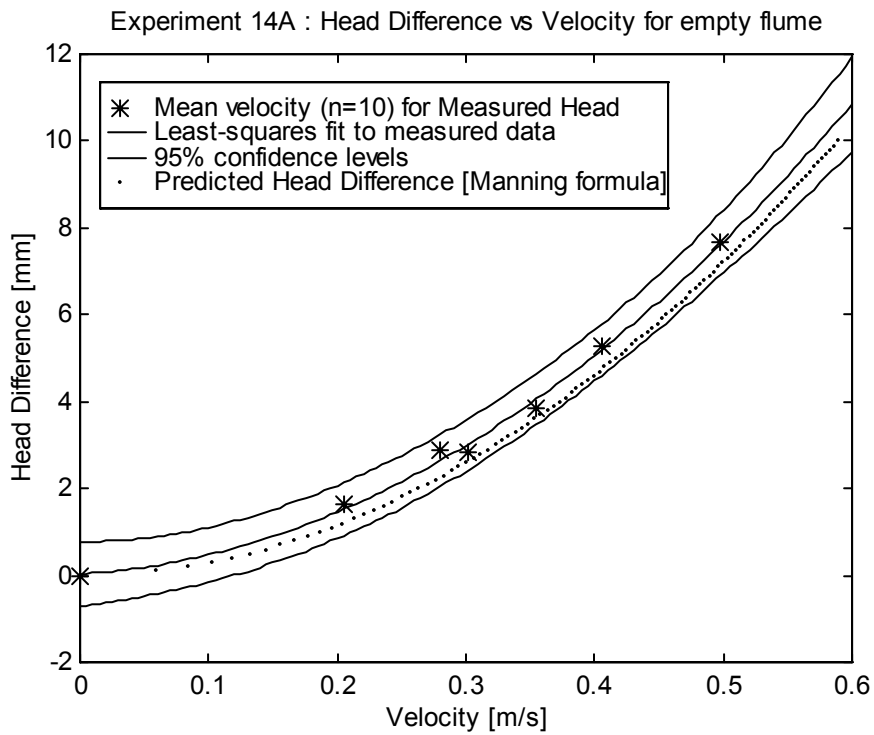


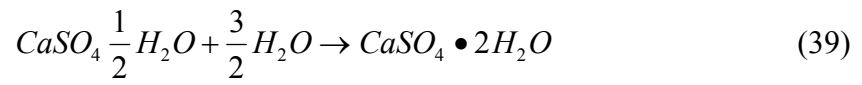
Figure 5. Measured and predicted head differences vs. velocity (Exp. 14A) for 9 meters of the empty flume.

Measurement of Mass Transport

The gypsum surfaces were prepared using US Gypsum No. 1 Pottery Plaster, a high quality plaster-of-paris used in the ceramics industry. The manufacturer gives typical chemical analysis (% by weight) of the plaster-of-paris powder as: 96.2% Beta-

Hemihydrate [CaSO₄•1/2H₂O], 0.5% Calcium Sulfate [CaSO₄], 2.4% Dolomite [CaMg(CO₃)₂], 0.4% Oxides, 0.5% Acid Insolubles. Analysis by Inductively-Coupled Plasma / Optical Emission Spectroscopy (ICP/OES) of a single sample of highly diluted US Gypsum No. 1 Pottery Plaster, dissolved in nitric acid, gave cation ratios for Ca:Mg:Na of 532:5.6:8. This is consistent with the manufacturer's analysis.

The plaster powder was hydrated using tap water in a 6:5 powder to water ratio by volume. The resulting reaction is:



The plaster was then mixed vigorously for approximately 2.5 minutes, and applied to the surface. The plaster was allowed to set overnight, before the experiment began.

The rates of dissolution of a variety of surfaces of different geometries were investigated. Smooth surfaces were prepared by pouring the plaster directly into the flume, and allowing it to set inside the flume. For the coral-rough surfaces, (Exp. 11 onwards) the coral skeletons were coated in plaster and allowed to set outside the flume (Fig. 6) before being placed in the flume at the beginning of each experiment. Coral reef skeletons were collected from the shoreline of Coconut Island, Kane'ohe Bay, Oahu, Hawaii, and soaked in tap water overnight before being coated with gypsum. The coral skeletons included *Porities compressa*, *Monitpora verrucosa* and *Fungia sp.* Soaking the coral skeletons in tap water reduced the possibility of seawater ions being released during the experiment, which would increase the conductivity of the water, causing error in calculation of calcium concentrations.

The roughness of the assemblage was determined by measuring the height of the skeletons above the flume bottom at 1 cm intervals along transects parallel to the flow (Fig. 3 & 7). Three, 200 cm transects (600 points) were measured. The height of the water column from the bottom, minus the average roughness height, k' , was used to determine the average height of the water over the sample. The standard deviation of the roughness height was used as an estimate of the roughness height (k_{σ}). The same coral skeletons were used for Exps. 11-19. A different set of coral skeletons were used for Exps. 20-21.

Time, temperature and conductivity were measured by a SEABIRD, Seacat 19 Profiler CTD. The CTD uses a Wein bridge-type oscillator to measure the conductivity of ions in solution at high frequencies. The high frequencies minimize the effects that ion-ion interactions have on conductivity measurement. This results in the near-linear relationship experimentally found between conductivity and calcium concentrations (Fig. 8). The SEABIRD software calculates specific conductance [$\mu\text{S cm}^{-1}$], which is the raw conductivity measurement, normalized to obtain the conductivity value that the same composition solution would measure at 25°C. It is important to note that the CTD measures at one position in the flume over time. Later in this section spatial variability will be inferred from a point measurement over time.

Figure 6. Coral-rough surfaces were made by plastering coral skeletons. The surfaces were allowed to dry overnight before placement in the flume.

Figure 7. Measurement of roughness height for coral-rough surface. The parallel rods 1 cm apart duplicate the surface profile, and facilitate easy measurement of roughness height.

Water samples were routinely taken at the beginning and end of the each experiment, as well as a number of times during the experiment. Samples were filtered using a GF/C glass-fiber filter, with a nominal pore size of 0.7 μm , and then refrigerated until analyzed. Samples were analyzed for calcium and other ions concentrations using a ICP/OES, and by potentiometric ion-selective electrode titrated with EGTA (Grasshoff et al., 1983).

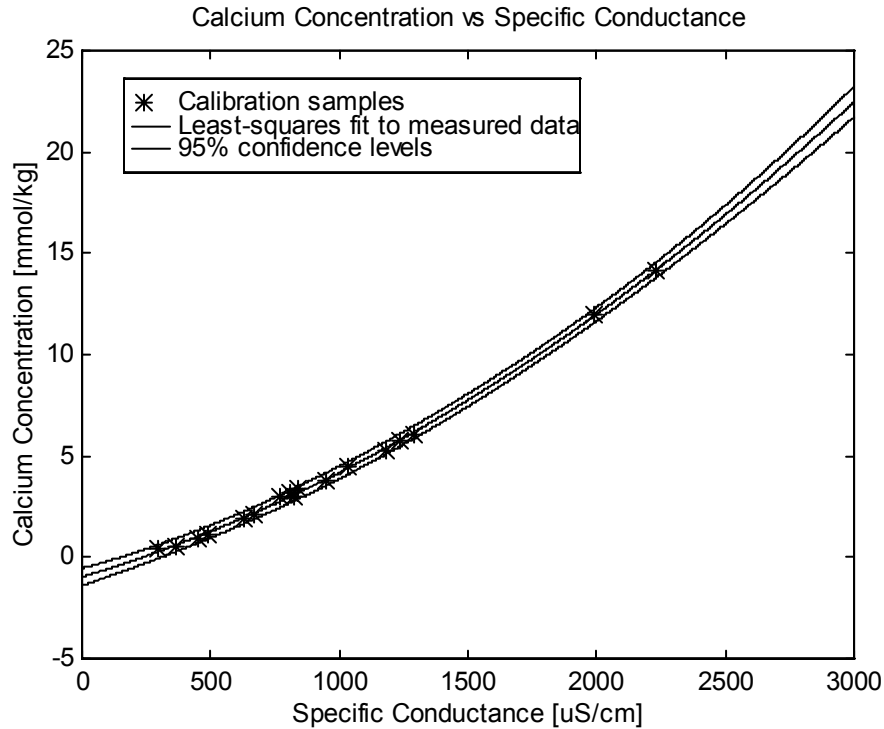


Figure 8. Calcium concentration measured by titration vs. specific conductance calculated from CTD measurement of conductivity [$\mu\text{S cm}^{-1}$] and temperature [K].

Samples were analyzed between a week and a few months after sampling. In all cases, the only cation to vary significantly in concentration over time was calcium, and was tightly correlated to the specific conductance measured at the time of sampling (Fig. 8). From the measured points a quadratic regression was developed, with 95% confidence levels shown. The points on this curve were taken from experiments over a six month

period; there were no significant changes in the CTD calibration or the quality of the plaster.

For each experiment, a curve of specific conductance vs. time was plotted (Fig. 9). This formed a logarithmic curve, as the conductance asymptotically approaches the saturation value. For low velocities, it is evident that there was considerable mixing time of the flume water before there was no spatial variability in concentration in the flume. The peaks in conductance are due to the higher concentration of ions in the volume of water which were exposed to plaster before circulation began. The peaks recur periodically as the volume of water initially exposed to the plaster passes the conductivity sensor. A polynomial fit is used to obtain the average concentration for the whole volume required

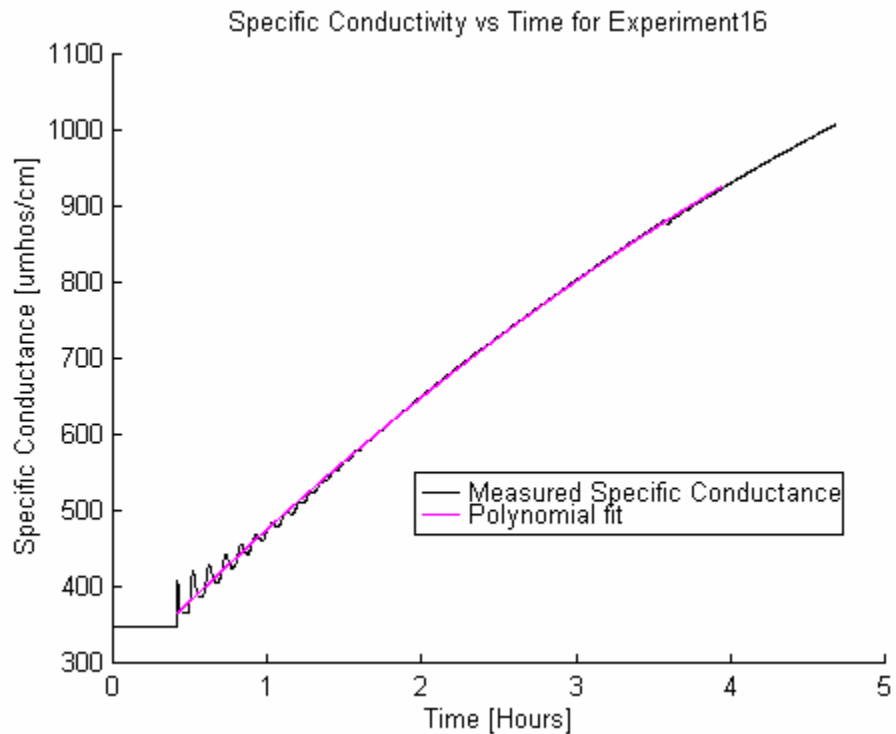


Figure 9. Specific conductance vs. time for Exp. 16. The corals were placed in the flume at time = 25 minutes. The initial peak is the first time the recirculating water that has been

exposed to the gypsum surface passes the sensor. The peak reoccurs about every 5 minutes, the time for one pass around the flume. Within 5 cycles, the flume is well mixed.

in Stanton number calculations.

An example of calculated Stanton numbers (Eq. 20) throughout a gypsum dissolution experiment for a smooth surface (Exp. 4) are shown in Fig. 10. Due to a changing ionic strength and temperature, both predicted and measured Stanton numbers change throughout an experiment. The reported Stanton numbers are an average of the 390 points shown in Fig. 10. The typical 95% confidence limit for a mean Stanton number is 1%. The largest error is due to a 5% error in the measurement of U_b and flume volume.

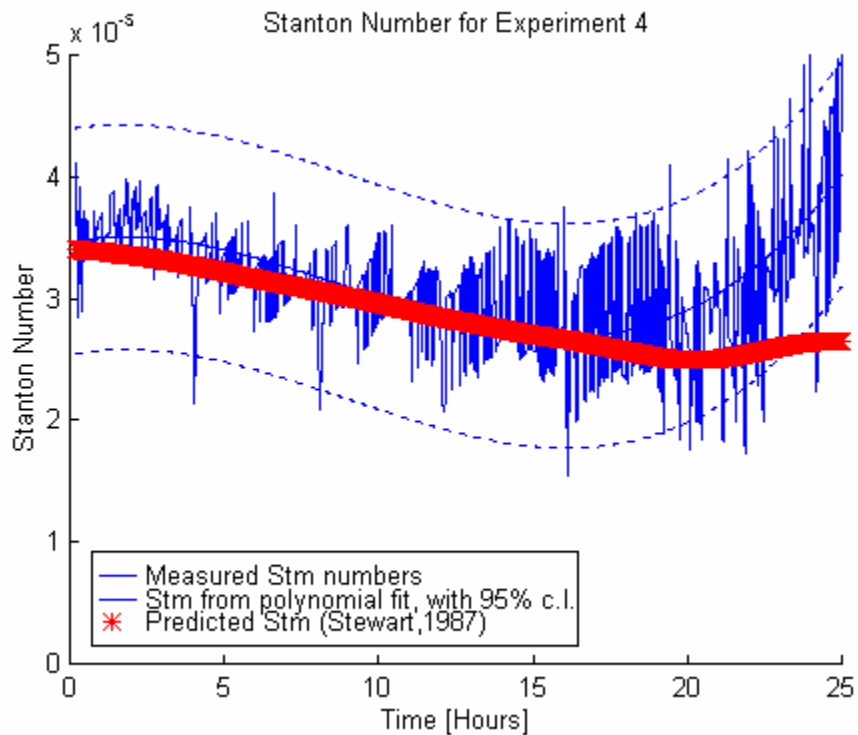


Figure 10. Stanton number for a smooth surfaces vs. time (Exp. 4). The prediction by Stewart (1987), Eq. 24 has been extrapolated to the lower Sc numbers of this experiment. After 15 hours the concentration gradient between the saturated wall and the near saturated water

approaches zero, resulting in the Stanton number (Eq. 20) becoming heading towards infinity. The reported results from all experiments will be within the first 5 hours.

The equipment, methods and calculations are now in accordance with the extensive engineering literature for both momentum and mass transfer characteristics for a smooth surface, and can therefore be confidently applied to coral rough surfaces (Dipprey and Sabersky, 1963).

Measurement of Mass Transport on Coral-rough Surfaces

The calculated rough St_m decreased because of a increase of bear surfaces as the gypsum dissolved. (Fig. 11; also Fig. 14 in results). Thus the reported St_m for each coral-rough gypsum surface was corrected to the initial measured value, when the surface was

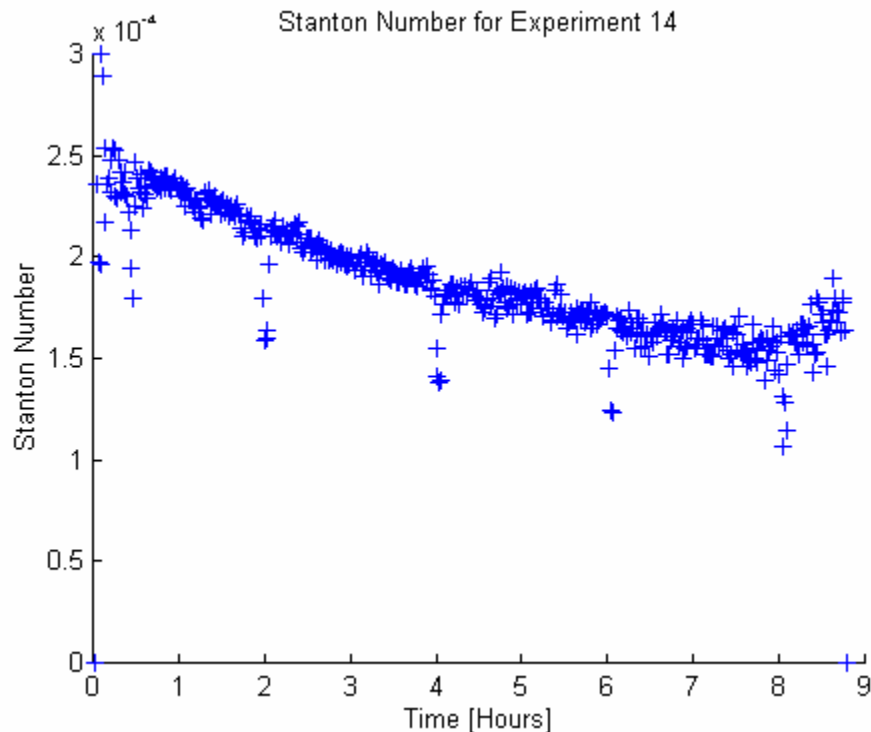


Figure 11. Measured Stanton numbers for a coral-rough surface (Exp. 14). $U_b = 0.32 \text{ m s}^{-1}$ for first 54 minutes. For the rest of the experiment, $U_b = 0.24 \text{ m s}^{-1}$.

fully coated. For example, when the velocity was changed in Exp. 14 at 54 minutes³, no step change occurred in St_m . For both velocities, St_m was taken to be 25×10^{-5} , the value recorded initially before the loss of surface area caused the slow decay from the initial value of 25×10^{-5} .

Experimental Outline

A few preliminary experiments were conducted (Exp. 1-3) to test the experimental equipment. Three smooth surface experiments (Exp. 4-6, Table 2) were then conducted to test the performance of gypsum dissolution against other mass-transfer limited chemical systems. Exp. 4 was conducted over a large temperature range, and therefore resulted in a large change in diffusivity. Exp. 5 used the same surface as Exp. 4, conducted eight days later, and at a variety of velocities. Exp. 6 involved the sand-papering of the new surface to create small roughness elements.

A variety of methods of creating rough surfaces were then tested (Exp. 7-10, 12). These surfaces resembled coral surfaces to varying degrees, notably a plaster smothered assemblage of coral skeletons (Exp. 9, Table 2), and a collection of randomly orientated triangular shapes (Exp. 12). Although the results of these experiments were representative of the surfaces themselves, the surfaces tested were not particularly good analogues for nutrient-uptake on coral reefs and thus are not included in the results.

The most successful replication of coral-rough surfaces was achieved by submerging coral skeletons in plaster-of-paris as the water-plaster mixture was hydrating

³ There is a step change in flux, but this is canceled out in the St_m calculation (Eq. 20) by the change in U_b .

(Exps. 11,13,14-17,19, 20F, 21A-B, Table 2). The setting speed of a six parts plaster, five parts water mixture allowed an approximately 2 minute "window" in which quickly submerged coral skeletons would be almost completely covered with an even, 0.5-2 mm thick of gypsum coat (Appendix D). These surfaces, with at least 95% of the surface coated, have been termed coral-rough gypsum surfaces. The gypsum was completely dissolved from each skeleton after experimentation, and the skeletons reused. The roughness of the two different assemblages was carefully analyzed during Exps. 15 and 16 (Fig. 12, Table 1) and Exp. 20.

At low velocities (Exp. 17), the pump's speed was not as consistent as at velocities above 0.05 m s^{-1} , and in fact the motor stalled on two occasions, but was immediately restarted. Pump reliability at low velocities was fixed for experiment 21A-B. Exp. 19 involved roughening the coral surfaces by the addition of plaster particles into the setting plaster mix, and further roughening with 60 grit sandpaper. Further roughening of the coral-rough gypsum surface was used to investigate whether small-scale roughness on the coral-rough gypsum surface enhances mass transfer.

Two experiments (Exp. 14A, 18, Table 2) were performed to determine the momentum characteristics of the empty flume (Exp. 14A) and the flume filled with coral skeletons (Exp. 18). By only measuring the momentum characteristics (velocity, head difference and height of flume), and not being concerned with dissolution characteristics, better precision was obtained.

Exp. 20 involved the direct comparison of ammonia uptake on a living coral community followed by the dissolution of gypsum from the same coral skeletons, placed in the same arrangement in the flume. Exps. 20A-D were ammonia-uptake experiments

from a coral assemblage in recirculated seawater, using the same procedures as Thomas and Atkinson (1996). The flume walls were scrubbed before each experiment, and the dirty seawater drained. The flume was refilled with Kane'ohe Bay seawater, and the corals left for 30 minutes in recirculating water. A 200 ml spike of 26 mM N as $(\text{NH}_4)_2\text{SO}_4$ was then administered evenly throughout the flume. The flume water continued to recirculate for a further 20 minutes, and then sampling begun. The water velocity was kept constant throughout the experiment. Eight to ten samples were taken over an eight hour period. Samples were siphoned from downstream of the community into a bucket for 25 minutes, to obtain an integrated concentration over the time period. The bucket was then sub-sampled using a 150 mL syringe, then filtered through a GF/C glass-fiber in-line filter and the sub-sample placed in a Nalgene bottle in a freezer within 5 minutes. NH_4 was measured using a Technicon II Autoanalyzer with modified standard Technicon industrial methods (Walsh, 1989). Exp. 20F was a control run, using the same methods as Exp. 20A-D, but without the coral community, to account for ammonia uptake by plankton and from the walls.

Exp. 20E used the same coral assemblage arranged identically, but the Stanton number was measured by gypsum dissolution using the techniques described for Exps. 11-19. Finally Exps. 21A and 21B, using gypsum dissolution of the assemblage of Exp. 20, involved a comparison of coral-rough and roughened coral-rough surfaces at low velocities.

Results

Momentum Transport on Coral-rough Surfaces

An example of coral-roughness is shown in Fig. 12 (Exp. 16). For the coral assemblage of Exps. 11-19, the mean height, k' , is 8.22 cm, and the standard deviation of the mean height, k_{σ} , is 4.8 cm (Table 1). For Exps. 20-21, $k' = 7.41$ cm, and $k_{\sigma} = 4.05$ cm.

Table 1. Topographical profile of the coral-rough assemblages used in Exp. 11-19, measured during Exps. 15 and 16. Transect positions were at 10, 20, and 30 cm from the left side of the flume if looking downstream.

Transect position	Experiment #15		Experiment #16	
	k' Mean Height [m]	k_{σ} Standard Deviation	k' Mean Height [m]	k_{σ} Standard Deviation
Left - 10 cm	0.0843	0.0504	0.0827	0.0493
Center - 20 cm	0.0782	0.0498	0.0662	0.0395
Right - 30 cm	0.0820	0.0478	0.0975	0.0504
TOTAL	0.0815	0.0493	0.0822	0.0483

Measured by volumetric displacement in a tank of known dimensions, the volume of the coral skeletons used for Exps. 11-19 was 27.0 ± 0.3 liters.

On surfaces with high roughness, Eq. 17 (Haaland, 1983) does not predict the friction coefficient measured in the flume (Fig. 13). This contrasts with smooth surfaces, for which the measured and predicted are similar (Fig. 5), indicating that engineering literature will not predict momentum transport at the high roughness of coral surfaces. However, the Haaland relation was developed from experiments at much smaller roughness height to water column height ratios than found in the flume (see Appendix B). The measured points in Fig. 13 are fitted to a cubic polynomial.

Experiment 16 : Topographical Profile

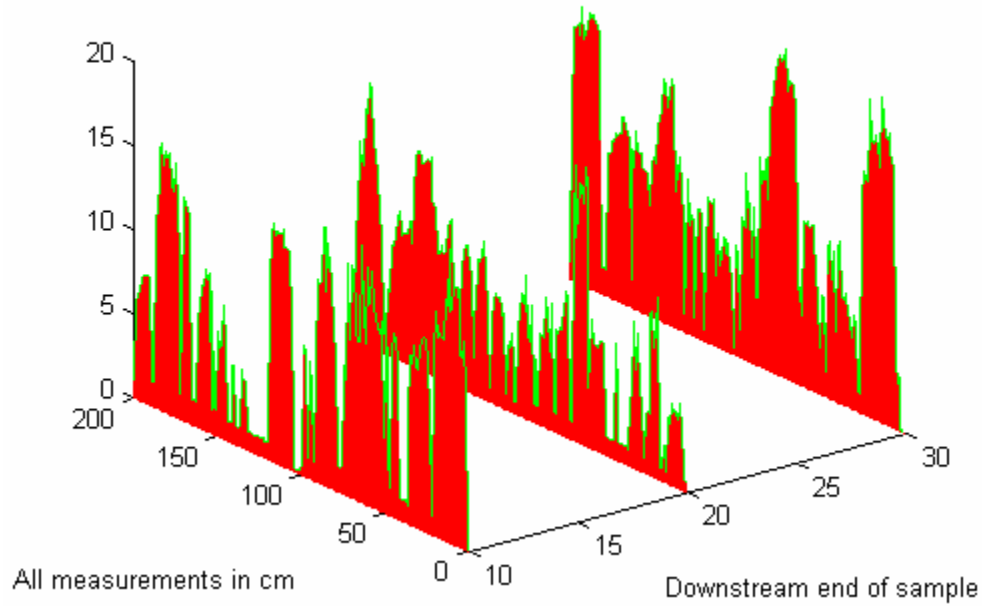


Figure 12. Roughness profile for Exp. 16. The mean height, k' , and standard deviation of the mean height k_σ , for the left, center and right (facing downstream) transects are listed in Table 1.

Mass Transport on Coral-rough Gypsum Surfaces

The plaster surfaces placed in the flume dissolved, releasing calcium and sulfate ions into solution, as expected. Fig. 14 shows the dissolution of the plaster from coral skeletons during Exp. 14 ($U_b \sim 0.3 \text{ m s}^{-1}$). The photographs are taken at the time the flow was started, 25 minutes, 45 minutes, and 17 hours later. The progressive photos of Fig. 14 show that the dissolution of plaster was not even on all surfaces, but instead tended to be removed more quickly at the tips of the corals (see Appendix D). During high flow rate conditions (above 0.1 m s^{-1}), the surface was visibly removed within an hour, and results obtained thereafter are from dissolution of a smaller surface area, as discussed in methods (Fig. 11).

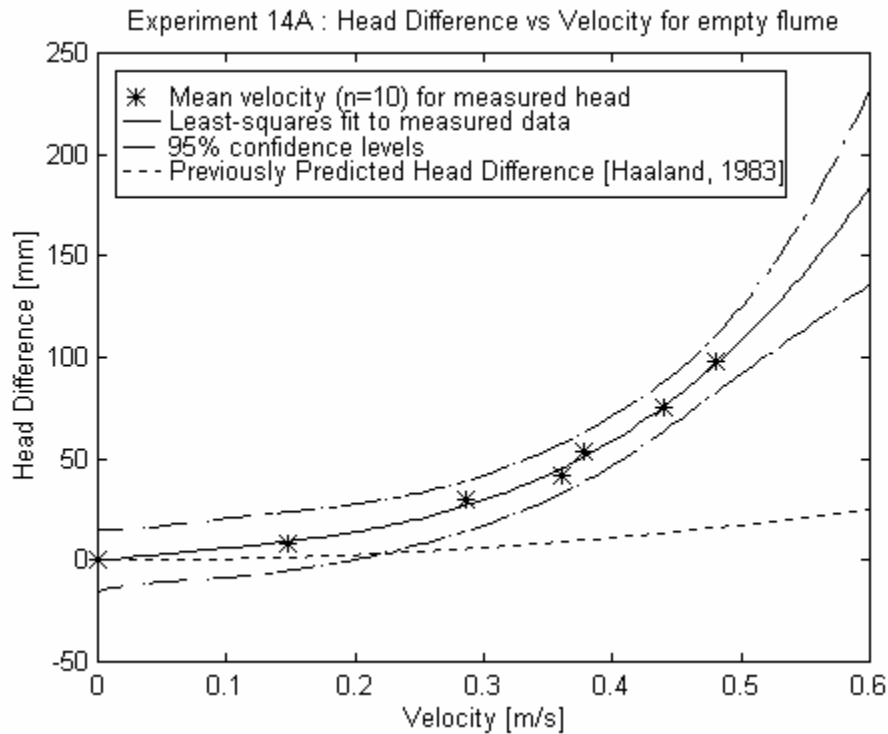


Figure 13. Predicted head difference over 9 m vs. head differences over 9 m calculated from the measured head differences over 2 m (Eq. 38).

St_m for smooth gypsum surfaces ranged between $2.6 - 3.5 \times 10^{-5}$ for varying temperature, ionic strength and bulk velocities above 0.1 m s^{-1} (Exps. 4-6, Table 2, Fig. 15). St_m for coral-rough gypsum surfaces ranged from $22 - 31 \times 10^{-5}$ at velocities greater than 0.1 m s^{-1} , an enhancement of 9 ± 1 over a smooth gypsum surface (Exps. 11,13-16, Table 2, Fig. 15). Much higher St_m numbers were measured for low water velocities (Exp. 17, Table 2, Fig. 15). Fine-scale roughening of a coral-rough gypsum surface does not increase mass transfer (Exp. 19 & 21, Table 2, Fig. 15). The St_m for coral-rough gypsum

- (i) Experiment 14, $t=0$, when water is just beginning to be recirculated.
- (ii) Experiment 14, $t=25$ minutes.

Figure 14. Experiment 14.

(iii) Experiment 14, $t=110$ minutes.

(iv) Experiment 14, $t=17$ hours.

Figure 14. (cont.) Experiment 14.

surface of Exps. 20-21 ranged from $17 - 19 \times 10^{-5}$, an enhancement of 6 ± 0.3 . The same enhancement was found from ammonia uptake experiments on the living coral community (Exp. 20B-D) over a theoretical smooth surface value.. Exp. 20-21 had a 10% lower k_{σ} than Exp. 11-19.

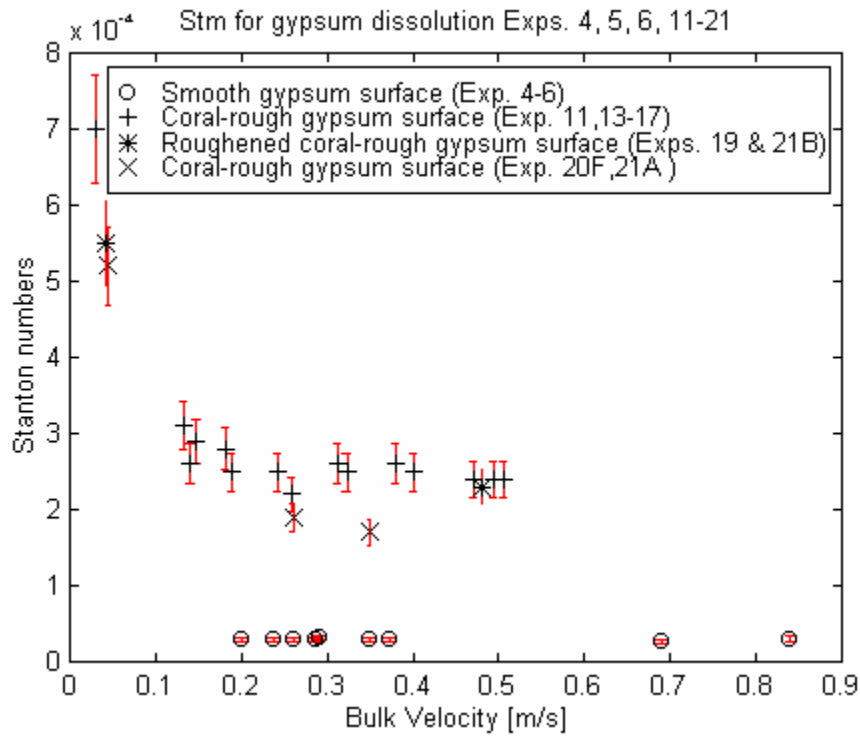


Figure 15. Stanton number, St_m vs. bulk velocity, U_b for gypsum dissolution Exps. 4-6, 11, 13-16, 17 and 19-21. Confidence intervals ($\pm 10\%$ of St_m) are based on the variation in measured bulk velocity ($\pm 5\%$) and height of the water ($\pm 5\%$) affecting St_m in Eq. 20. Exp. 11-19 are from one set of coral skeletons, and Exp. 20-21 from another, less rough (smaller k_{σ}) assemblage.

Table 2. Summary of experimental results. The same coral skeletons were used for Exps. 11-19. The living corals from Exp. 20B-D were used for Exps. 20E, 21A-B. St_m and Sc are for gypsum dissolution unless stated. Coral skeletons evenly coated with gypsum are referred to as coral-rough. The roughened coral-rough surfaces (Exps. 19 & 21B) refer to coral-rough surfaces further roughened with sandpaper to create randomly-orientated 1 mm grooves on coral-rough surface. Smothered coral rubble of Exp. 9 referred to coral-rubble coated with plaster in the flume. The reported results of Exp. 20B-D include correction for uptake on flume surfaces measured by Exp. 20F.

Exp. No.	Roughness	U_b [m/s]	c_f ($\times 10^{-3}$)	Sc^*	St_m ($\times 10^{-5}$)
4	Smooth	0.29	7.28	1300 - 2100	3.5-3.0
5	Smooth	0.20	7.95	1360	2.9
		0.24	7.61	1360	2.9
		0.26	7.45	1370	2.9
		0.29	7.31	1370	2.9
		0.37	7.10	1380	2.9
6	Sandpaper 1500 and 60 grit	0.35	see Exp. 14A	1360	2.9
		0.84		1410	3.0
		0.69		1440	2.6
9	Smothered coral rubble	0.19	140	1300-2000	20
11	Coral-rough	0.14	see Exp. 18	1250	26
		0.38			
13	Coral-rough	0.50	see Exp. 18	1270	24
		0.47			24
		0.51			24
		0.40			25
		0.31			26
14	Coral-rough	0.32	see Exp. 18	1290	25
		0.24		1340	25
14A	Smooth (velocity and c_f measurements only)	0.21	0.0084	-	-
		0.28	0.0080	-	-
		0.30	0.0068	-	-
		0.36	0.0067	-	-
		0.41	0.0070	-	-
		0.50	0.0068	-	-
15	Coral-rough	0.13	see Exp. 18	1260	31
		0.18		1270	28
		0.15		1280	29
16	Coral-rough	0.19	see Exp. 18	1320	25
		0.26		1340	22
17	Coral-rough	0.030	see Exp. 18	1260	70
18	Coral-rough	0.15	0.1065	-	-
		0.29	0.1003	-	-

	(velocity and c_f measurements only)	0.36 0.38 0.44 0.48	0.0886 0.1046 0.1085 0.1182	- - - -	- - - -
19	Roughened coral-rough	0.48	see Exp. 18	1260	23
20B - D	Ammonia uptake by living corals	0.24 0.30 0.30	0.041 0.042 0.040	475 475 475	31 31 39
20E	Coral-rough	0.26 0.35	0.050 0.043	1300 1350	19 17
20F	Ammonia uptake by empty flume	0.20	see Exp. 14A	475	34
21A	Coral-rough	0.045	0.233	1230	52
21B	Roughened coral-rough	0.043	0.207	1240	55

Table 2 (cont.).

Discussion

Momentum Transport

The largest random error in all measurements in this study was due to the turbulent nature of the flow. An average water velocity, U_b , was calculated from 10 drogue measurements. While individual measurements were accurate, in a randomly fluctuating medium a finite sampling provides only an approximation of the true average. This error was greater on rough surfaces, where turbulence was greater and velocity gradients steeper. A comparison with the literature values (Fig 5, John and Haberman, 1988) for smooth surfaces, and the repeatability of measurements on rough surfaces (Table 2), show the errors were on the order of $\pm 5\%$ or less, as would be indicated by the variability in the measurement of velocity.

The measurement of the height of volume of water in the flume was made difficult by evaporation during an experiment, the slope on the flume bottom (up to 15 mm difference in height), as well as the slope created by friction. The height measurement was also important for friction coefficient, c_f , calculations. An error of up to $\pm 5\%$ is estimated due to miscalculation of volume.

The variability seen in the experimental curve fitting of velocity to head difference (Fig. 13) was of the same magnitude as would be expect from the error in the measurement of bulk velocity and volume. The measured values do not vary by more than $\pm 10\%$ from the plotted cubic fit. Considering the strong correlation between friction coefficient and mass transfer, the same variability is to be expected in mass transfer results as well.

As stated in the introduction, Bilger and Atkinson (1992) suggest that corals may possess an enhancement mechanism unexplained in engineering literature. As pointed out by Thomas and Atkinson (1996), and illustrated in Fig. 13, the calculated friction factors, c_f , from Haaland (1983) and used by Bilger and Atkinson, are low. The higher friction factor measured on coral skeletons must be due to geometric differences between engineering surfaces and coral-rough surfaces. Thus it should be expected that in a turbulent flow, for a mass-transfer limited chemical, enhanced c_f will result in an enhanced St_m .

Mass Transport

The photographs in Fig. 14 show the plaster being removed from the coral skeleton surface. The dissolution of gypsum, as described in the background section, experimentally showed a velocity dependence. It also had Stanton numbers of the same magnitude, and temperature and ionic strength dependence, of other chemicals for smooth surfaces found in the literature (Steward, 1987). Furthermore, in an independent study of gypsum dissolution on a smooth, rotating disk, Barton and Wilde (1971) conclude that the dissolution of gypsum is mass transfer limited. Therefore, as the dissolution of gypsum is mass transfer limited, it is a good experimental analogue for the flux of chemical species to and from a coral-rough object. Thus the St_m from the dissolution of gypsum from a coral-rough surface can be compared to the St_m for the uptake of ammonia and phosphorus to live coral reef communities.

Fig. 14 illustrates some qualitative aspects of the flux of chemical species to and from a coral-shaped object. The transport rate is not even on the surface, but is greater

at points of faster local velocity, such as on the tips (see Appendix D). A greater removal rate is also observable from delicately branched coral skeletons, which probably induce more turbulence.

Other Mass Transfer Studies on Coral-rough Surfaces

Table 3 lists a number of mass transfer studies on coral-rough surfaces. The studies of Thomas and Atkinson (1996) and Larned and Atkinson (1996) provide the basis for comparison of coral-rough gypsum surfaces to live coral communities.

The measured St_m of different chemical species is a function of Sc of the species, Re_k and c_f . (Dipprey and Sabersky, 1963). To compare St_m of gypsum to the St_m of ammonia from geometrically similar surfaces (and therefore Re_k and c_f), St_m can be scaled according to the ratio obtained from Eq. 24 (Bilger and Atkinson, 1995). For the same Re_k and c_f :

$$\frac{St_{m,ammonia}}{St_{m,gypsum}} = \frac{0.0575Sc_{ammonia}^{-2/3} + 0.1184 / Sc_{ammonia}}{0.0575Sc_{gypsum}^{-2/3} + 0.1184 / Sc_{gypsum}} \cong 2 \quad (40)$$

Table 3. Data analysis of experiments undertaken on coral-rough surfaces for a variety of chemical species and flow conditions. Atkinson and Bilger (1992) gave c_f values, but they were calculated, not measured, and have since been questioned by Thomas and Atkinson (1996).

Environment	Chemical (Sc number*)	U_b [m/s]	Re_k	c_f	Re ($\times 10^3$)	St_m ($\times 10^{-5}$)
Kane'ohe Bay barrier reef (Bilger and Atkinson, 1992)	phosphate (~1340)	0.1 1.0	230 - 2000	0.010 - 0.026	425 4,250	average 170
Uniform flow experimental coral community (Atkinson and Bilger, 1992)	phosphate (~1340)	0.0229- 0.581	313 - 7900	not measured	15.9 - 403	13.8- 106
Enewetak Atoll reef flats (Atkinson, 1992)	phosphate (~1340)	not given	not given	not measured	not given	185 - 370
Uniform flow experimental <i>Porites compressa</i> (Thomas and Atkinson, 1996)	ammonium (~475)	0.48 0.06 0.06 0.29 0.51 0.57	not given	not given	not given	19 94 88 32 19 20
Uniform flow experimental. (PC) (Thomas and Atkinson, 1996)	ammonium (~475)	0.039 0.225 0.375	853 3766 5208	0.264 0.158 0.109	43.6 249 414	185 43.1 38.4
Uniform flow experimental. (PD) (Thomas and Atkinson, 1996)	ammonium (~475)	0.036 0.115 0.207 0.296	501 1129 2093 2986	0.126 0.063 0.067 0.063	39.9 127 229 326	108 58.3 54.1 37.6
Uniform flow experimental. (HR)	ammonium (~475)	0.09 0.238 0.277	1015 2687 3262	0.101 0.102 0.111	100 263 306	54.4 37.4 41.5
Uniform flow experimental. (LR) (Thomas and Atkinson, 1996)	ammonium (~475)	0.033 0.084 0.189 0.308	107 276 581 935	0.052 0.053 0.047 0.045	36.2 92.5 208 340	48.4 60.7 36.0 36.7

Table 3 (cont.). Data analysis of experiments undertaken on coral-rough surfaces for a variety of chemical species and flow conditions.

Uniform flow gypsum coral shapes	gypsum (1200-1400)	0.03 - 0.506	700 - 5400	0.06 - 0.5	-	22-70
Dictyosphaeria (Larned and Atkinson, 1996)	ammonium (~475)	0.02 - 0.12	700 - 1200	0.03 - 0.45	-	45 - 170

Eq. 40 is used to scale the $St_{m,gypsum}$ to $St_{m,ammonia}$ (Fig. 16), the result being that measured $St_{m,gypsum}$ is multiplied by two to account for the slower diffusion of gypsum relative to ammonia. Now a direct comparison of St_m for ammonia uptake on a coral community and coral-rough gypsum surface can be made (Fig. 16).

The similar magnitude of the St_m of a live coral community and a coral-rough gypsum surface is proof that the mechanism of mass transfer enhancement is geometric rather than biological. Furthermore, since the coral-rough surfaces did not possess the fine scale roughness of living coral, and yet had the same magnitude of St_m , the geometric features responsible for enhancement are all large scale. The similar dissolution rate of the roughened coral-rough gypsum surface (Exp. 19 & 21) to unroughened coral-rough gypsum surfaces also illustrates this point. Small-scale phenomena (Fig. 4, k_1 - k_4) such as a fractal surface, are not responsible for the enhancement of mass transfer on coral-rough surfaces.

Mass Transfer on Coral-rough Surfaces

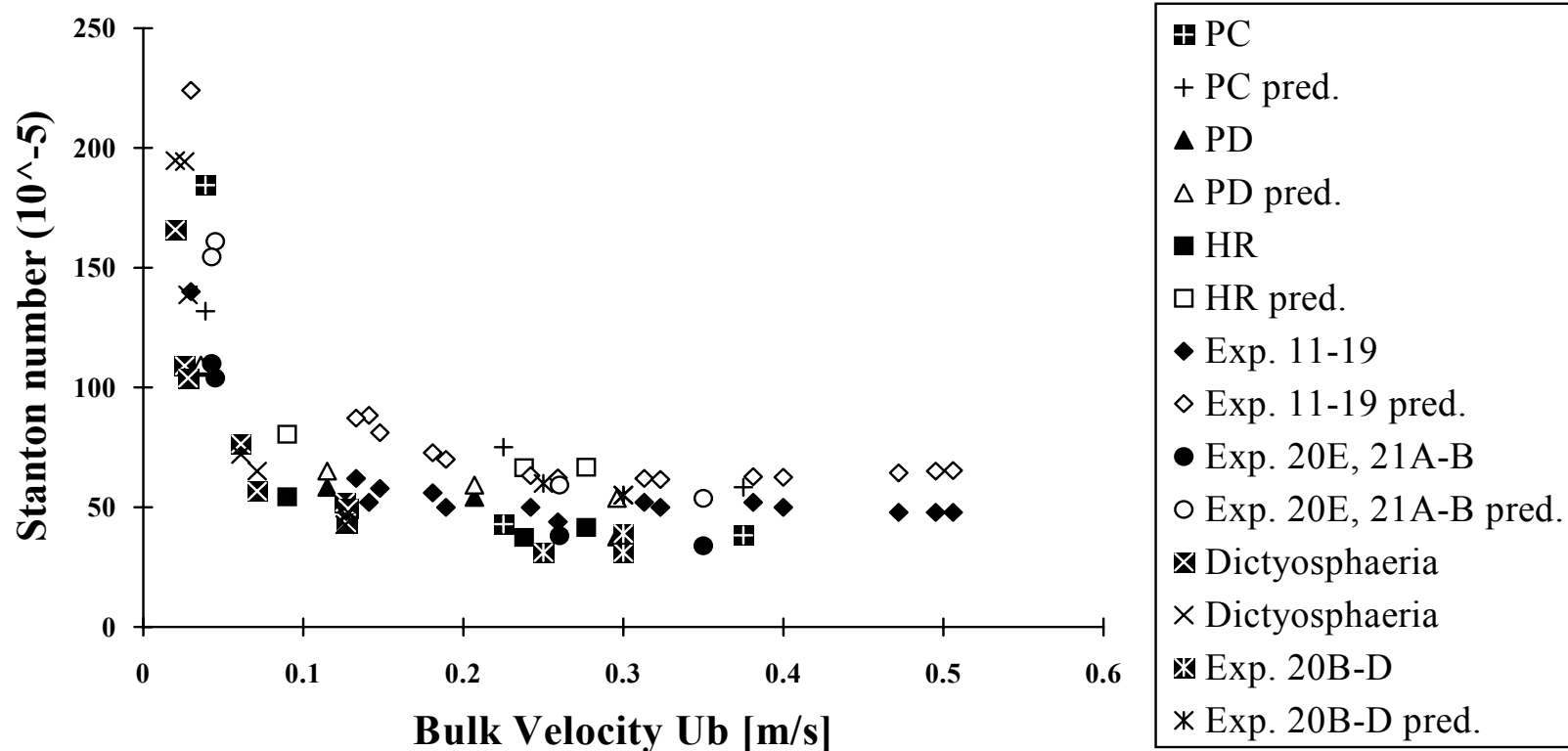


Figure 16. A comparison of mass transfer on coral-rough surfaces. Shaded symbols are measured values; outlined symbols are predicted values using Dipprey and Sabersky, 1963 with $C = 5.19$, and using the standard deviation of the roughness height, k_σ , as the roughness height. *Porites compressa* (PC), *Pocillopora damicornis* (PD), and HR (high relief rubble) (Thomas and Atkinson, 1996), Dictyosphaeria (Larned and Atkinson, 1996) and Exp. 20B-D were measured using the uptake of ammonia. Exp. 11-19 and Exp. 20E, 21A-B were measured from gypsum dissolution from coral-rough surfaces.

As pointed out earlier in the discussion, Bilger and Atkinson (1992) cited the work of Dipprey and Sabersky (1963), but incorrectly calculated the mass transfer because they underestimated the friction coefficient (Thomas and Atkinson, 1996). Fig. 13 shows the measured head difference over a coral surface compared to the predicted value used by Bilger and Atkinson for their mass transfer calculations. The Dipprey and Sabersky (1963) study involved the investigation of heat transfer from sand-roughened pipes. The geometric similarity between pipes and channels has already been shown, as well as the fact that both heat and mass transfer are examples of diffusion along chemical potential gradients.

Dipprey and Sabersky chose sand-grain roughness to "simulate natural roughness" because of its "three-dimensional nature and the random shape of the roughness elements." Dipprey and Sabersky's correlation Eq. 36-37 uses a coefficient of 5.19 for St_k^{-1} . Fig. 16 is a graph of the predicted Stanton numbers (Eq. 36-37) for the data of this study, Thomas and Atkinson (1996), and Larned and Atkinson (1996), plotted with the measured values for these respective studies.

Dipprey and Sabersky point out that the coefficient of 5.19 (Eq. 37) is a function of the type of roughness. Replacing 5.19 with 7.0 for coral-roughness (Fig. 17) provides an excellent agreement between predicted values and the measured values of Thomas and Atkinson (1996), this study, and from *Dictyosphaeria* (Larned and Atkinson, 1996). The fact that changing the Dipprey and Sabersky coefficient to 7.0 improves both the prediction of living coral surfaces and coral-rough gypsum surfaces is further evidence that the format

Mass Transfer on Coral-rough Surfaces

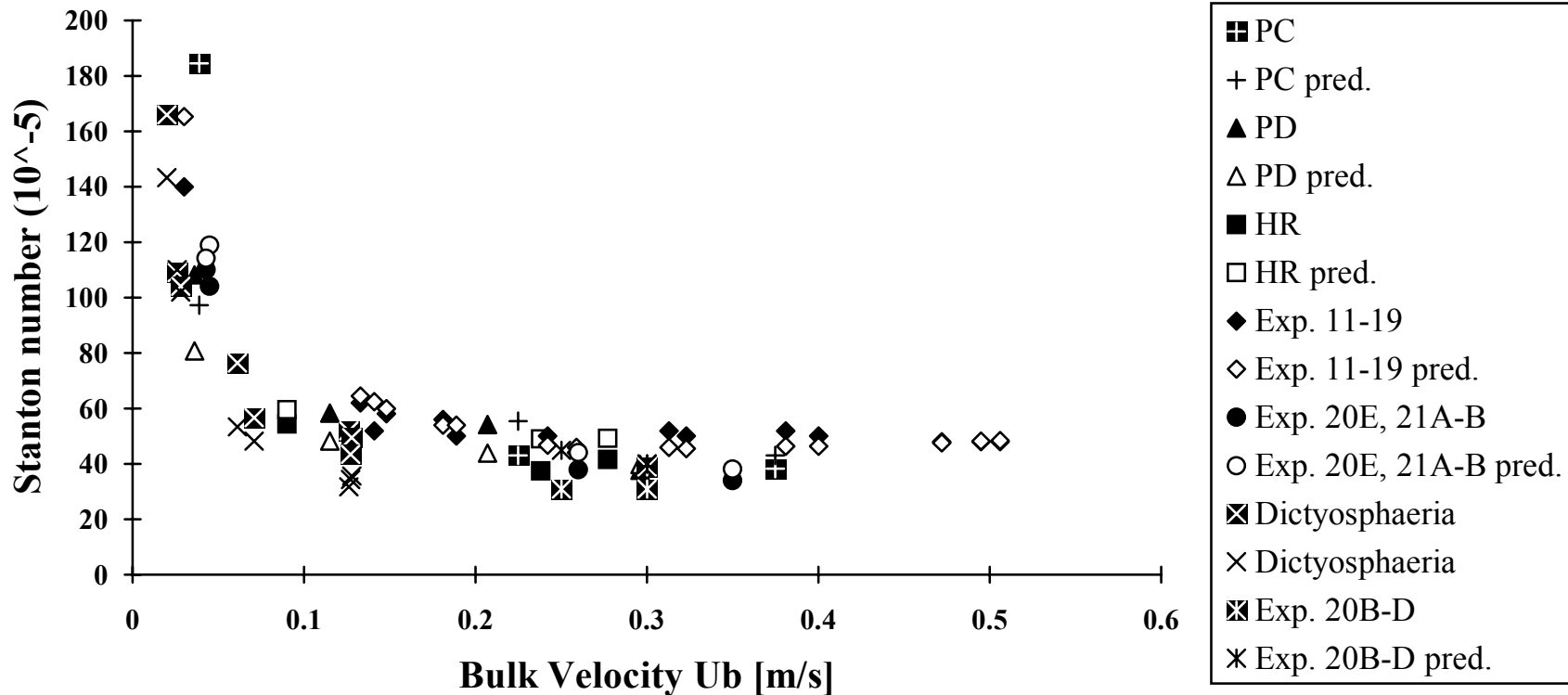


Figure 17. A comparison of mass transfer on coral-rough surfaces. Shaded symbols are measured values; outlined symbols are predicted values using Dipprey and Sabersky, 1963 with $C = 7.0$, and using the standard deviation of the roughness height, k_σ , as the roughness height. *Porites compressa* (PC), *Pocillopora damicornis* (PD), and HR (high relief rubble) (Thomas and Atkinson, 1996), Dictyosphaeria (Larned and Atkinson, 1996) and Exp. 20B-D were measured using the uptake of ammonia. Exp. 11-19 and Exp. 20E, 21A-B were measured from gypsum dissolution from coral-rough surfaces.

of Dipprey and Sabersky's heat transfer correlation is valid for coral-rough surfaces. Since Dipprey and Sabersky's correlation uses only geometric parameters (and not biological ones), this is further grounds for quantifying mass transfer rates in terms of geometric and not biological variables.

The predicted St_m of Dipprey and Sabersky's (1963) correlation modified for coral-roughness does not correlate well below 0.1 m s^{-1} . However, the correlation is empirically determined from rough surfaces in which c_f does not change with Re : a phenomena described in engineering literature as the momentum boundary layer being fully rough. Below 0.1 m s^{-1} , c_f increases with Re on coral-rough surfaces (Thomas and Atkinson, 1996), and the boundary layer is considered transitional (Kays and Crawford, 1993). Therefore, Dipprey and Sabersky's modified relationship is only useful on coral-roughness for velocities above 0.1 m s^{-1} . Further study may determine why flow over coral-roughness is transitional at Re_k of up to 1000 ($U_b \sim 0.1 \text{ m s}^{-1}$), an order of magnitude higher than on sand-grain roughness and other engineering surfaces.

Implications for Coral Reef Ecology

The results of this thesis support Atkinson and Bilger's (1992) assertion that the diffusion of nutrients to coral reefs is mass transfer limited, the mechanism of limitation being diffusion through the diffusive sublayer. Bilger and Atkinson's (1992) field observations yield a Stanton number for phosphate of at least 1.7×10^{-3} . To compare the Stanton number from a uniform flow to an oscillatory flow such as seen in a wave-driven environment, a correction factor must be included (Appendix A). For the field conditions

Mass Transfer on Coral-rough Surfaces

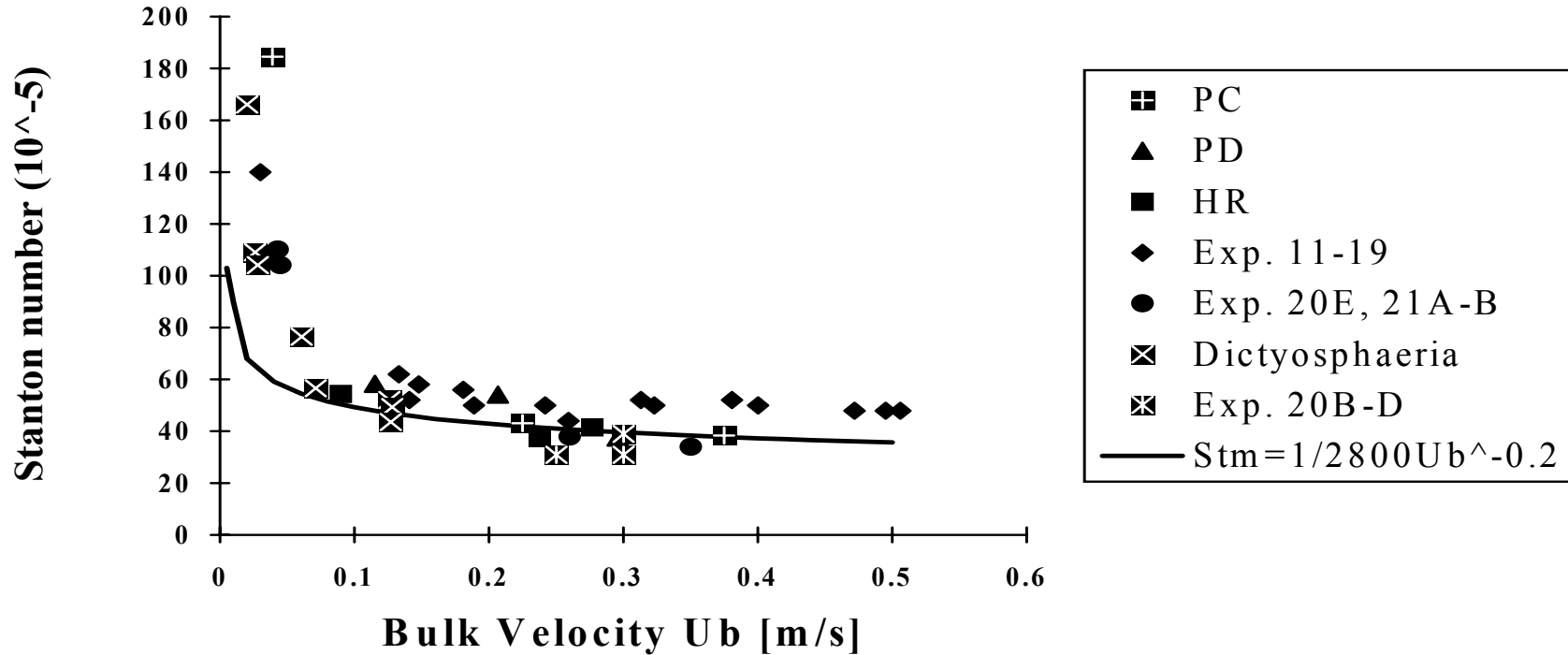


Figure 18. A comparison of mass transfer on coral-rough surfaces to a common relation of St_m vs. U_b for smooth and grooved surfaces. Measured points as per Fig. 17-18. The constant, $k = 1/2800$, has been chosen so St_m has the same magnitude as coral-rough surfaces.

described by Bilger and Atkinson (1992), this factor is 3.2. Therefore using the uniform flow, coral-rough results obtained in this study, we can say that $2.5 \times 10^{-4} \times 3.2 = 0.8 \times 10^{-3}$ can be accounted for by geometric enhancement of mass transfer in a oscillatory flow. A factor of two remains unaccounted.

The results of this study show that corals have a morphology that is highly effective at extracting nutrients from the water column. Fig. 18 presents the measured results of Fig. 17, along with a curve fitting the data of the form $St_m = kU_b^{-0.2}$, where k is a constant. This form of relationship is observed on smooth and ordered-rough surfaces such as grooves. Note the enhancement of coral-rough surfaces at low velocities above that of engineering surfaces. This enhancement may be explained by the following ecological arguments.

Competition will be strongest when resources are scarce. Under these conditions, adaptations are expected to be more refined by natural selection. For nutrient uptake, the scarce availability of nutrients occurs at low velocities, and it is at low velocities we see the strongest trend away from ordered rough surfaces (Fig. 18). Therefore, it is reasonable to argue that coral morphology is highly adapted for the uptake of nutrients at low velocities.

A counter argument, however, would suggest that the coral morphology is highly adapted to survival in a wave swept environment, where structural integrity is of the utmost importance. As we have already learned, the friction factor, c_f , is a measure of the shear stress (and hence force) exerted by the water on the coral, and c_f and St_m are strongly correlated. So to protect themselves from injury, the corals must reduce c_f , thereby reducing St_m , effectively trading off between survival and nutrient uptake.

Or has natural selection sidestepped this "trade off?" Survival in a wave swept environment need only be considered at high velocities, and nutrient uptake becomes increasingly important at low velocities. It is my hypothesis, therefore, that coral-rough shapes are highly adapted to both nutrient uptake at low velocities, and survival in a wave-swept environment at high velocities.

My argument is further strengthened by considering the importance of roughness on an individual organism, as opposed to the whole community. At low velocities the flow is less turbulent. The presence of a particular roughness element results in significantly more turbulence (and therefore higher c_f) in the vicinity of the element. At high velocities, the flow is much more turbulent, and there is only a small increase in turbulence about the vicinity of a particular roughness element. A coral that increases c_f at low velocities will therefore primarily affect its own uptake rate. At high velocities, however, turbulence created by the whole community tends to dominate, as flow over one organism is highly altered by its neighbors. A type of roughness that results in a higher c_f at high velocities will have little additional benefit to the individual in nutrient uptake. As a result, we see the high velocity St_m following the trend (although not magnitude) of regular engineering surfaces.

A corollary to the above arguments must be provided to explain the variety of different coral-rough morphologies that thrive in coral reefs. Thomas and Atkinson (1996), along with Larned and Atkinson (1996), show that a variety of different species, with different rough morphologies, follow the same St_m vs. U_b curve (Fig. 18). A wide range of coral-rough morphologies appear capable of obtaining the highly adapted

performance exhibited in Fig. 18. This is one factor in allowing the diversity of rough morphologies for which coral reefs are cherished.

A particular coral species can also exhibit more than one morphology, depending on the environment in which it grows. To what extent are coral morphologies controlled by environmental factors? The evidence of faster dissolution rates from the tips of coral-rough gypsum surfaces (Appendix D) raises the possibility that a branching structure could develop as a result of the tips receiving more nutrients, and therefore the length of the branch grows faster than the diameter.

A Changing Boundary Layer

Diffusive fluxes, such as those of nutrients and other chemicals beneficial or harmful to corals, are strongly dependent on water velocity and temperature. Sea surface temperature and local weather patterns are predicted to vary with global climate change (Steering Committee of the Climate Change Study, 1995). For example, a change from 22°C to 25°C in sea surface temperature will decrease kinematic viscosity by ~ 6% and increase diffusivity of NH_4^+ by ~ 7%, resulting in a decrease in Sc number of 12%. Using Eq. 24, this results in a increase in Stanton number of NH_4^+ of 8%. To assess the effects of increased uptake of nutrients on coral communities, growth rates of different species at elevated nutrient uptake rates must be assessed. It may well be found that an algae such as *Dictyosphaeria* fares better with higher uptake rates than historically more established species.

As introduced earlier, naturally rough surfaces are ubiquitous in nature. Throughout the oceans, and other ecosystems, many chemical systems appear never to

reach equilibrium, but are instead kinetically controlled. The results from this study may be applicable to other naturally rough surfaces that are mass transfer limited. Naturally rough inorganic surfaces are capable of at least 9 ± 1 times the flux of a smooth surface, and may be subject to significant variations with changing global climate patterns.

Industry efficiency relies heavily on transport phenomena, particularly heat exchange and heat recovery. The usefulness of a heat exchange surface is often assessed by plotting the ratio of heat transfer to friction dissipated (St/c_f) against Reynolds number. This gives an indication, at a specified Re , whether the addition of roughness to a smooth surface "costs" more in friction dissipated than the gain in heat transfer. The same analysis can be done for mass transfer to coral-rough surfaces (Fig. 19). At $2 \times 10^5 < Re < 5 \times 10^5$ ($U_b = 0.2-0.5 \text{ m s}^{-1}$), there is a marginal gain in mass transfer over friction loss, compared to a smooth surface. Similar size gains are of great interest to engineers (Dipprey and Sabersky, 1963).

Fouling, however, is a problem that must be overcome before the application of coral-rough surfaces in industrial processes becomes a possibility. Fouling occurs when a surface becomes coated by constituents of the flow that stick to the heat transfer surface, reducing heat transfer and often increasing pressure drop through constriction of flow. Living coral communities, incidentally, overcome the problem of fouling through the action of grazers on the coral surface.

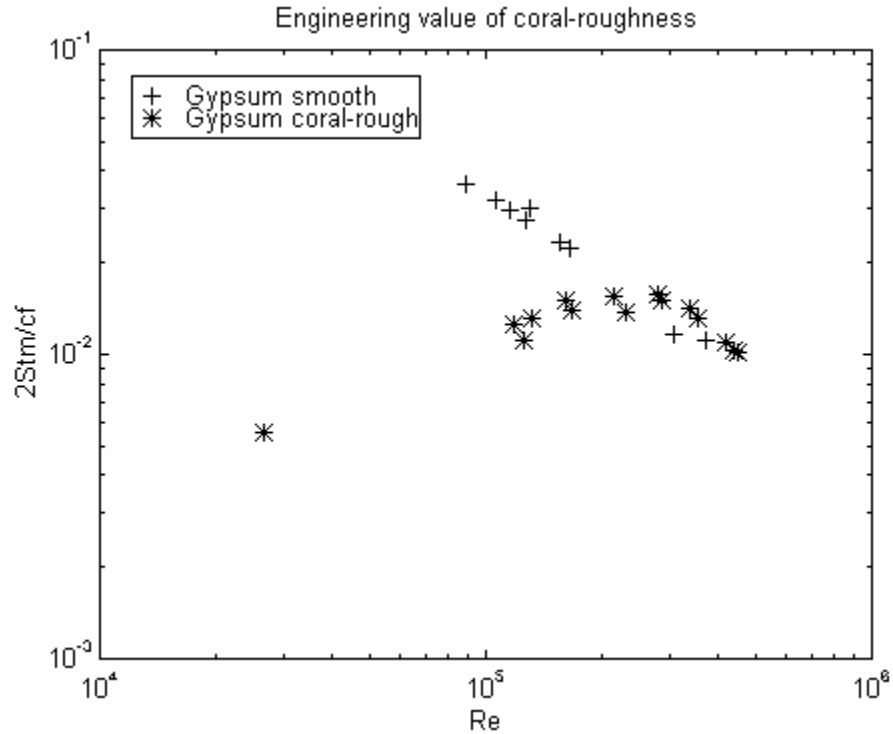


Figure 19. The engineering value of mass (or heat) transfer from a coral-rough surface, as shown by the normalized flux (St_m) normalized to friction dissipated (c_f) plotted over a range of the flow conditions quantified by the Reynolds number (Re). Presented results for smooth surfaces are from Exps. 4-6, and for coral-rough surfaces are from Exps. 11-19.

Returning briefly to coral ecology, Fig. 19 quantifies the ecological arguments given earlier in the discussion. The most "cost-effective" mass transfer on coral-rough surfaces occurs at between $0.20\text{-}0.50\text{ m s}^{-1}$. In this range, nutrient uptake is required, but risk of injury introduces a "cost" for the corals. Below 0.20 m s^{-1} , the "cost" diminishes, as the ocean provides the energy, and there is little risk of injury. As a result, coral-rough surfaces are *designed* for maximum efficiency at velocities above 0.20 m s^{-1} , and, at low velocities, maximum mass transfer at any "cost."

Conclusions

1. The dissolution of coral-rough gypsum surfaces proved to be an effective experimental analogue for investigating chemical fluxes to and from live coral communities.
2. Coral-rough gypsum surfaces had fluxes (as measured by the Stanton number) of between $17 - 70 \times 10^{-5}$, depending on the water velocity, friction factor and roughness height of the assemblage. The enhancement of mass transfer over that of a smooth surface is up to 9 ± 1 times, and is similar to that observed for phosphate and ammonia uptake on a variety of experimental coral communities.
3. The similar mass transfer characteristics of coral-rough gypsum surfaces and a living coral community is due to similar large scale geometric features such as branching. Neither active biological mechanisms nor small scale phenomena such as fractal geometry affect mass transfer rates on living coral communities.
4. The Atkinson and Bilger (1992) model of nutrient uptake, using the rate limiting step of fluxes resulting from diffusion through the boundary layers, is valid. Such models may be useful tools for understanding chemical fluxes on reef systems in future environments of altered sea surface temperature and weather patterns.
5. Coral-roughness has probably arisen through natural selection to maximize the uptake of nutrients at low velocities, and to increase survival at high velocities in a wave swept environment.

References

- ATKINS, P. W. 1994. Physical Chemistry (5th Ed.). Oxford University Press.
- ATKINSON, M. J. 1992. Productivity of Enewetak Atoll reef flats predicted from mass transfer relationships. *Cont. Shelf Res.* **12**: 799-807.
- ATKINSON, M. J., AND R. W. BILGER. 1992. Effects of water velocity on phosphate uptake in coral reef-flat communities. *Limnol. Oceanogr.* **37**: 273-279.
- ATKINSON, M. J., E. KOTLER, AND P. NEWTON. 1994. Effects of water velocity on respiration, calcification and ammonium uptake of a *Porites compressa* community. *Pac. Sci.* **48**: 296-303.
- BAIRD, M. E. 1992. Mass Transfer on rough surfaces at high Schmidt numbers in a circular couette flow. B.E.(Hons) thesis, Dept. of Mech. Eng., Uni. of Sydney.
- BARTON, A. F. M., AND N. M. WILDE. 1971. Dissolution rates of polycrystalline samples of gypsum and orthorhombic forms of calcium sulphate by a rotating disc method. *Fara. Soc. Trans.* **67**: 3590-3597.
- BOUDREAU, B. P., AND N. L. GUINASSO, JR. 1978. The influence of diffusive sublayer on accretion, dissolution and diagenesis at the seafloor. p115-145. *In* K.A. Fanning and L.T. Markeim [eds.], *The dynamic environment of the ocean floor*. Lexington.
- BILGER, R. W., AND M. J. ATKINSON. 1992. Anomalous mass transfer of phosphate on coral reef flats. *Limnol. Oceanogr.* **37**(2): 261-272.
- BILGER, R. W., AND M. J. ATKINSON. 1995. Effects of nutrient loading on mass transfer rates to a coral-reef community. *Limnol Oceanogr.* **40**(2): 279-289
- CORBETT D. 1990. Mass transfer in pipe flow at high Schmidt number with high surface roughness. BE Thesis, Dept. of Mech. Eng., Uni. of Sydney.
- CONLEY, D. C. AND D. L. INMAN. 1992. Field observations of the fluid-granular boundary layer under near-breaking waves. *J. Geophy. Res.* **97**: 9631-9643.
- CONLEY, D. C. AND D. L. INMAN. 1994. Ventilated oscillatory boundary layers. *J. Fluid Mech.* **273**: 261-284.
- DADE, W. B., 1993. Near-bed turbulence and hydrodynamic control of diffusional mass transfer at the sea floor. *Limnol. Oceanogr.* **38**(1): 52-69.
- DARWIN, C. R., 1906. *The voyage of the Beagle*. Everymen's Library.

- DAWSON, D. A. AND D. TRASS. 1972. Mass transfer at rough surfaces. *Int. J. Heat Mass Transfer* **15**: 1317-1336.
- DEAN., R. G., AND R. A. DALRYMPLE. 1984. *Water wave mechanics for engineers and scientists*. Prentice-Hall, Inc.
- DIPPREY, D. F., AND D. H. SABERSKY. 1963. Heat and momentum transfer in smooth and rough tubes at various Prandtl numbers. *Int. J. Heat Mass Transfer* **6**: 329-353.
- FURNAS, M., A. W. MITCHELL, AND M. SKUZA. 1995. *Nitrogen and Phosphorus Budgets for the Central Great Barrier Reef Shelf*. Res. Pub No. 36. Great Barrier Reef Marine Park Authority.
- GRIFFOLL, J., X. FARRIOL, AND F. GIRALT. 1986. Mass transfer at smooth and rough surfaces in a circular couette flow. *Int. J. Heat Mass Transfer* **29**: 1911-1918.
- GRASSHOFF, K., M. EHRHARDT, AND K. KREMLING. 1983. (2nd Ed.) *Methods of Seawater Analysis*. Verlag Chemie.
- GROSS, T. F., AND F. E. WERNER 1994. Residual circulations due to bottom roughness variability under tidal flows. *J. Phys. Oceanogr.*, **24**: 1494-1502.
- GUTFINGER, C. [ed.]. 1975. *Topics in transport phenomena*. Hemisphere Publishing Corporation.
- HAALAND, S. E 1983. Simple and explicit formulas for the friction factor in turbulent pipe flow. *J. Fluid Eng.* **105**: 89-90.
- HARDIE, L. A. 1967. The gypsum-anhydrite equilibrium at one atmosphere pressure. *Am. Min.* **52**: 171-200.
- HERRERO, J., F. X. GRAU, J. GRIFOLL AND F. GIRALT. 1991 A near wall k- ϵ formulation for high Prandtl number heat transfer. *Int. J. Heat Mass Transfer* **34**: 711-721.
- HERRERO, J., F. X. GRAU, J. GRIFOLL AND F. GIRALT. 1993. The effect of grid size in near wall k- ϵ calculations of mass transfer rates at high Schmidt numbers. *Int. J. Heat Mass Transfer* **37**: 882-884.
- KAYS, M. W., AND M. E. CRAWFORD. 1993.(3rd Ed.) *Convective heat and mass transfer*, McGraw-Hill.

- INCROPERA, F. P., AND D. F. DE WITT. 1990. Fundamentals of heat and mass transfer, 3rd ed. John Wiley & Sons Inc.
- JOHN, J. E. A., AND W. L. HABERMAN. 1988. (3rd Ed.) An introduction to fluid dynamics. Prentice Hall.
- JOHNSON, L. E. 1994. Enhanced settlement on microtopographical high points by the intertidal red alga *Halosaccion glandiforme*. Limnol. Oceanogr. **39**(8): 1893-1902.
- JUMARS, P. A., AND A. R. NOWELL. 1984. Fluid and sediment dynamic effects on marine benthic communities. Am. Zool. **24**: 45-55.
- LARNED, S. AND M. J. ATKINSON. 1996. Contribution of water column nutrients to the growth rates of coral reef macroalga *Dictyosphaeria cavernosa*: Effects of water velocity on ammonia and phosphate uptake. Manuscript in prep.
- LEE, B. E., AND B. F. SOLIMAN. 1977. An investigation of the forces on three dimensional bluff bodies in rough wall turbulent boundary layers. J. Fluids. Eng. pp503-510.
- LUKERSKY, P. 1992. An investigation of the sources of high enhancement of mass transfer in coral reef communities. B.E. thesis. Dept. of Mech. Eng., Uni. of Sydney.
- LI, Y., AND S. GREGORY. 1974. Diffusion of ions in sea water and deep-sea sediments. Geochem **38**: 703-714.
- MUNK, W. H., AND G. A. RILEY. 1952. Absorption of nutrients by aquatic plants. J. Mar. Res. **11**: 215-240.
- NIKURADSE, J. 1933. Laws for flow in rough pipes. Forsch. Arb. Ing.-Wes., Nr 361.
- PESKIN, C. S., AND D. M. McQUEEN. 1995. A general method for the computer simulation of biological systems interacting with fluids. In: C.P. Ellington & T.J. Pedley [eds.]. Biological Fluid Dynamics: 265-276. The Company of Biologists Limited.
- RAUPACH, M. R., AND A. S. THOM. 1981. Turbulence in and above plant canopies. Annu. Rev. Fluid Mech. **13**: 97-130.
- REYNOLDS, A. J. 1975. The prediction of turbulent Prandtl and Schmidt numbers. Int. J. Heat Mass Transfer **18**: 1055-1069.
- SCHLICHTING, H. 1955. Boundary Layer Theory. McGraw-Hill.
- SELMAN, R. J., AND C. W. TOBIAS. 1978. Mass transfer measurement by the limiting-current technique. Adv. Chem. Eng. **10**: 211-318.

STEERING COMMITTEE OF THE CLIMATE CHANGE STUDY. 1995. Climate change science: current understanding and uncertainties. Australian Academy of Technological Sciences and Engineering.

STEWART, W. E. 1987. Forced convection: Asymptotic forms for laminar and turbulent transfer rates. *AICHE J.* **23**: 28-37.

TANTIRIGE, S., AND O. TRASS. 1984. Mass transfer at geometrically dissimilar rough surfaces. *Can J. Chem. Eng.* **62**: 490-496.

THOMAS, F. I. M., AND M. J. ATKINSON. 1996. Friction coefficients and roughness of coral reefs: estimates of mass transfer limited uptake of ammonia. In press.

WALSH, T. W. 1989. Total dissolved nitrogen in seawater: a new high temperature combustion method and a comparison with photo-oxidation. *Mar. Chem.* **26**: 295-311.

WEBER, H. E. [ed.]. 1979. *Turbulent Boundary Layers*. American Society of Mechanical Engineers.

WHITFIELD, M., AND D. JAGNER. 1981. *Marine Electrochemistry*. John Wiley & Sons Inc.

Other Sources

Plasters and Gypsum Cements for the Ceramic Industry. United States Gypsum Company.

Glossary

Activity (a): An experimental measure to represent the 'effective' mole fraction of chemical. Activity corrects for the non-ideal behavior of ions, due to phenomena such as ion-ion interactions.

Bulk velocity (U_b): The velocity measured by a neutrally buoyant drogue traveling over the sample area. U_b will be the integrated velocity of the fluid in contact with all of the drogue's surfaces over the measurement time interval.

Chemical potential of i (μ_i): The rate of change in total Gibb's free energy with respect to the change in quantity of chemical species i, while keeping pressure, temperature and the ratio of the quantity of other chemical species constant.

Coral-rough: Phase termed for this study to refer to surfaces of similar roughness to coral communities.

Diffusive sublayer: The inner portion of the momentum boundary layer where the transport of a chemical species is by diffusion down chemical potential gradients.

Friction coefficient (c_f): Dimensionless measure of shear stress exerted on a fluid by a surface, arising from both form drag and skin friction.

Friction (or shear) velocity (u_*): A characteristic velocity used to represent the velocity within the momentum boundary layer.

Form drag: A stress exerted on a fluid by a protruding shape interrupting the flow, including effects such as the stress created by the wake of a protruding shape.

Fully rough: A condition of a flow where, due to surface roughness, the friction coefficient becomes independent of Reynolds number. Generally occurs at $Re_k > 70$,

although on a coral-rough surface transition to fully rough behavior does occur until a much higher Re_k .

Head: Pressure measured as the equivalent height of water at the prevailing hydrodynamic conditions (salinity, temperature, atmospheric pressure).

Hydraulic diameter (D_h): A calculated dimension shown to correlate the momentum transport behavior of different flow geometries, such as an open channel and a pipe.

Hydraulically smooth: A surface whose c_f and St_m are those of a smooth surface. Generally observed on surfaces at $Re_k < 5$, but not investigated for coral-rough surfaces.

Mass-transfer limited: The rate limiting step for transport of a chemical species from a fluid to a surface is diffusion through the diffusive sublayer.

Momentum boundary layer: The region of flow where velocity changes from the wall velocity to 99% of the free stream velocity.

Plaster-of-paris: Commercial name for the mined gypsum ($CaSO_4 \cdot 2H_2O$). Also known as alabaster.

Prandtl number (Pr): Ratio of molecular diffusivity of momentum to the molecular diffusivity of heat.

Reynolds number (Re): Ratio of viscous forces to inertial forces. It is a measure of the likelihood of a fluid to be laminar or turbulent.

Reynolds roughness number (Re_k): Nondimensional measure of the surface roughness, based on either the average roughness height, k' , the standard deviation of roughness height, k_σ , or the equivalent sand-grain roughness height, k_s .

Sand-grain roughness height (k_s): The mesh dimension of a sieve used to sort sand-grains by Nikuradse (1933) for friction dissipation experiments. An equivalent sand-grain

roughness (also k_s) has since been defined (Schlichting, 1955) to give a roughness dimension to other shapes observed to have the same friction characteristics as the sand-grains of Nikuradse of dimension k_s .

Schmidt number (Sc): Ratio of molecular diffusivity of momentum to molecular diffusivity of a chemical species.

Sherwood number (Sh): Dimensionless flux of a chemical species.

Skin friction: A shear stress exerted on a fluid by a surface parallel to the flow.

Specific Conductance: The calculated conductance for an solution, as would be measured at 25°C. The units of $\mu\text{S}/\text{cm}$ or $\mu\text{mhos}/\text{cm}$ are equivalent to $\mu\Omega^{-1}\text{cm}^{-1}$.

Stanton number (St_m): Ratio of the uptake of a substance to the advection of that substance past the uptake surface.

Thermodynamic Force (F): A theoretical force (per mole) defined so as to oppose the work per unit distance done by random molecular motion in a chemical potential gradient.

Transitional roughness: Flow behavior intermediate between hydraulically smooth and fully rough. Generally occurs at $5 < Re_k < 70$, although seen at much higher Re_k on coral-rough surfaces.

Turbulent Schmidt number (Sc_t): The ratio of eddy diffusivity of momentum to the eddy diffusivity of a chemical species, and approximately equal to one.